A MECHANICAL APPARATUS TO QUANTIFY THE REFLEX RESPONSE OF THE HUMAN HEAD/NECK SYSTEM

By

GERALD QUINLAN LUCAS

A thesis submitted in partial fulfillment of
the requirements for the degree of

MASTER OF SCIENCE IN MECHANICAL ENGINEERING

WASHINGTON STATE UNIVERSITY
School of Mechanical and Materials Engineering

DECEMBER 2006

To the Faculty of Washington State University:

The members of the Committee appointed to examine the thesis of GERALD QUINLAN LUCAS find it satisfactory and recommend that it be accepted.

_____
Chair

_____

_____

ACKNOWLEDGMENTS

This research could not have been completed without the blessings of the Lord Almighty or the extreme helpfulness and support of my advisor, Dr. Anita Vasavada. Of nearly equal importance was the encouragement of my family and friends throughout this, especially Melissa who pushed me to continue to work even when I did not want to.

Drs. David Lin and David Hutton were extremely helpful in various parts of my thesis and their feedback was much appreciated. Within the lab, Kasey Schertenleib began the work on this project and must be thanked for his part as well. I would also like to thank Liying Zheng, Richie Lasher, Jonathan Danaraj, and Sampath Gollapudi for their help with testing my equipment. Anne Margreet-Knottnerus worked with me on the final parts of this project and will continue my work in the future. The other people at the Lin-Vasavada lab were large helps in lab meetings and brainstorming for my project.

A MECHANICAL APPARATUS TO QUANTIFY THE REFLEX RESPONSE OF THE HUMAN HEAD/NECK SYSTEM

Abstract

By Gerald Quinlan Lucas, M.S.M.E.
Washington State University
December 2006

Chair: Anita Vasavada

The human head/neck system is a rotational, biological model that can be represented as an inverted pendulum and approximated as a second order system. The central nervous system responds reflexively to external perturbations by activating the neck muscles to return the head to neutral position. This study consisted of 3 parts. A device to examine the reflexive response of the human head/neck system was built and tested. An inverted pendulum was tested to verify that the methods will identify the system parameters of an inverted pendulum. Finally, 2 human subjects were tested with the device to determine the muscle onset latencies and kinematics for the head/neck system following a perturbation to the head.

The motion in the frame designed for this experiment was less than 1% of the motion of the force applicator during trial runs and thus proved sufficiently stiff to meet our requirements.

The inverted pendulum's system parameters were identified by a second order model. The estimated stiffness averaged a 6% error when compared with the known spring stiffness. The damping coefficient was consistent throughout the trials.

The human subject results showed that, for our experiment, the head/neck system should not be approximated as a second order system. It demonstrated a brief period of second order vibrations but did not oscillate about its initial position. The maximum head motions showed different results between subjects and perturbation directions. Subject 1 moved more when their head was pushed forward while subject 2 moved more when their head was pushed back.

The muscle onset latencies (time between force onset and muscle activation) averaged between 20 and 90 ms. These were within the range of other studies' results. Subject 1 showed no statistically significant difference in onset latencies between forward and backward perturbations. Subject 2 showed differences in most of their muscle onset latencies between directions. This suggests a different response in forward versus backward motion.

Overall, we achieved our goals. This study allows other investigators to continue the testing later with more subjects under different conditions. This will lead to a better understanding of the control of the human head/neck system.

TABLE OF CONTENTS

Page

LIST OF TABLES

LIST OF FIGURES

CHAPTER ONE

INTRODUCTION

The human head/neck system is a rotational, biological system which is often described as an inverted pendulum and approximated as a second order system [1, 2, 3]. When the head is accelerated, the central nervous system controls the responses of the neck muscles to stabilize the head in space. The active neck muscles, along with various passive biological tissues, thus supply the stiffness and damping properties of the head and neck. We wish to quantify the stiffness and damping coefficients of the head/neck system as well as the activation onset latencies, the delay between force application and muscle activation, for the neck muscles.

The goals for this study are as follows:

1. Develop an experimental setup which will allow for perturbations to be safely applied to a seated subject's head in any direction in the horizontal plane.
2. Use this system to verify methods for estimating the stiffness and damping properties of an inverted pendulum.
3. Use this system to study the reflex response and characterize the stiffness of the human head/neck system in flexion and extension.
4. Use this system to determine the onset latencies for major neck muscles.

In order to accomplish these goals, we first built a frame which allowed for perturbations to be delivered to the head in any direction in the horizontal plane. Next, we tested the stiffness of the frame to ensure that it would not interfere with our experiments. We then built and tested a second order system (inverted pendulum) to establish that we could use our system to characterize an inverted pendulum. Finally, we used this system to apply a

force to the head in order to determine the stiffness, damping coefficient, and neck muscle onset latencies for humans.

There are differing reasons for performing this study. The head neck system is a complex system containing many different muscles spanning multiple joints. This complexity gives the nervous system many different ways to stabilize the head and neck. By studying neck muscles' reflex responses, we hope to come to a better understanding of how the nervous system uses reflexes and muscles to stabilize the head.

As with any biological system, modeling the head and neck mathematically would lead to a greater understanding of the system. Characterizing the response of the head and neck system in healthy subjects will also provide baseline data for future studies evaluating neck stiffness and reflex response in persons with disorders of the head and neck musculoskeletal system such as whiplash injury or vestibular deficit.

Although other researchers have studied the head/neck system, most have not applied perturbations directly to the head but rather accelerated the body, thus causing the head to move. Studies where the head was directly perturbed have mostly focused on the onset latencies of the neck muscles. Our study is unique because we will apply the perturbations directly to the head and then allow the head to move freely in response to the perturbations rather than having a continuously applied force. We will then use these data to determine the stiffness and onset latencies for the head/neck system.

The following sections contain a basic overview of the human neck anatomy as well as a description of how muscles work and the different reflexes associated with head stabilization. Previous studies are then reviewed followed by a basic overview of second order identification techniques. A brief overview of the various devices used in this

study is then presented. Finally, the methods, results, and discussion for each of the three experimental parts (natural frequency of the frame, characterization of an inverted pendulum, and human subject testing) are presented.

CHAPTER TWO

BACKGROUND

As background for this study, various anatomical and physiological principles must be understood. These include the basic makeup of the human neck, how muscles work, and the reflexes involved in control of head position. Other studies have examined the reflex responses of the human neck, so a basic overview of what has previously been accomplished is presented as well as any findings which influence this study. Since the main objective of this study is to identify certain parameters in an inverted pendulum, a brief overview of how this is accomplished is presented.

2.1 ANATOMICAL PLANES

The human body is generally divided by three planes (Figure 2.1.1). The sagittal plane divides the body into right and left sections, the frontal or coronal plane divides it into front and back, and the horizontal or transverse plane divides it into top and bottom sections.

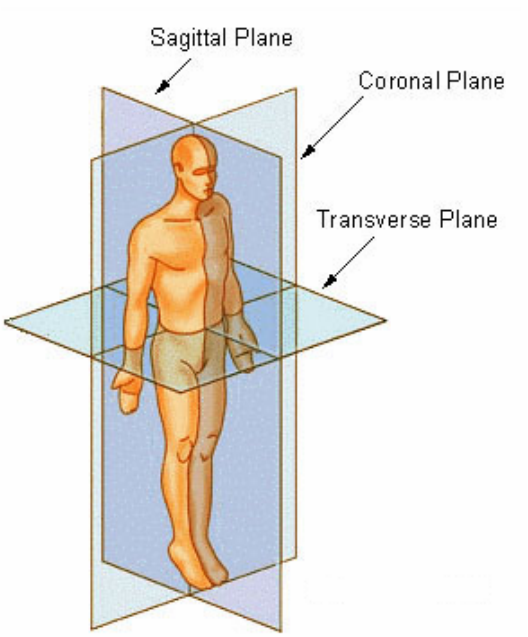

FIGURE 2.1.1 Anatomical planes of the human body [4]

We can use these planes to define the three basic motions which the head undergoes (Figure 2.1.2). Extension and flexion, looking up and down respectively, are rotations in the midsagittal plane. These movements are also called pitch. Axial rotation or yaw is rotation in the horizontal plane, i.e. turning the head left or right. Lateral bending or roll is rotation in the frontal plane, i.e. tilting the head to the side. Although most head movements do not correspond directly to one of these primary motions, we can define the motions by a combination of the primary motions.

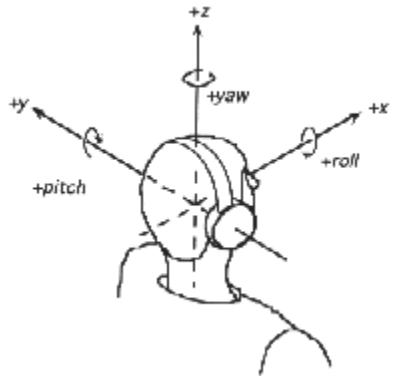

FIGURE 2.1.2 Basic motions of the human head [5]

2.2 ANATOMY OF THE NECK

The human neck is also known as the cervical region of the spine (Figure 2.2.1). It is composed of 7 vertebrae: C1 is the uppermost cervical vertebra and attaches to the base of the skull; C7 is the lowest cervical vertebra and attaches to T1, the first vertebra in the thoracic region (upper back). Between each of these vertebrae is soft tissue called an intervertebral disc. The discs help to cushion the spine, support compressive loads, and absorb energy. Vertebrae are also connected via ligaments which provide passive stabilization. Muscles attach to the vertebrae via tendons and provide force for both stabilization and movements of the neck. Both ligaments and tendons are passive tissues; they do not actively generate forces like muscles do but can only resist applied forces and motions.

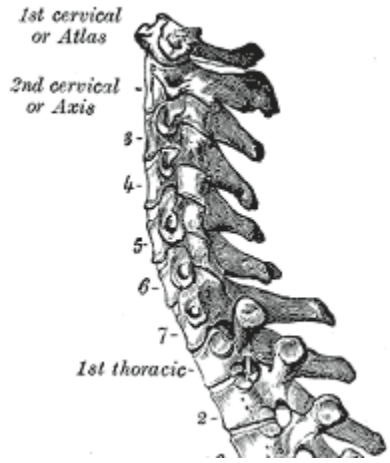

FIGURE 2.2.1 Cervical region of human spine [6]

Cervical vertebrae (Figure 2.2.2) consist of a body and several processes. The body is the cylindrical part of the vertebra. The spinal cord runs through the canal behind body. There are two types of processes, transverse and spinous. The transverse processes protrude from the sides of the vertebra. The spinous process protrudes from

the back of the vertebra and can be seen under the skin surface in the lower cervical spine. Muscles attach to the transverse and spinous processes, providing increased lever arms.

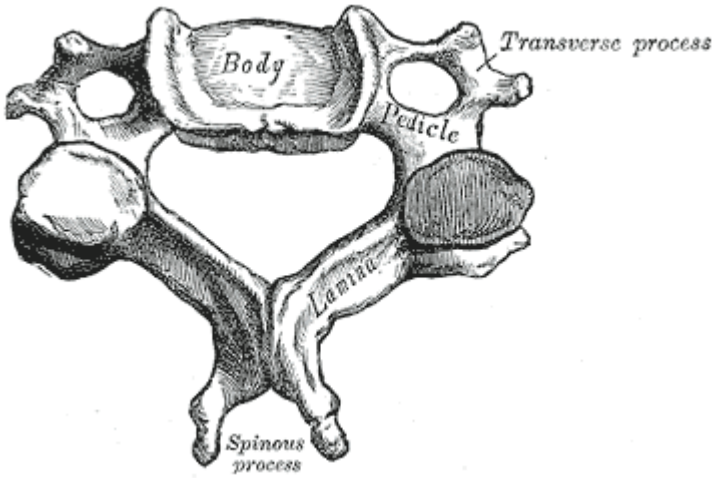

FIGURE 2.2.2 Typical cervical vertebra [6]

There are over 20 pairs of muscles in the human neck. However, in this study we will focus on four muscles which are commonly studied in neck studies. These are the sternocleidomastoid (SCM), the trapezius (TRAP), the splenius capitis (SPL), and the semispinalis capitis (SEMI). They are the most commonly studied because they represent the majority of the isometric moment generating capacity in the neutral position [7] and are some of the most superficial, close to the skin, muscles. The sternocleidomastoid runs from the sternum and clavicle (collar bone) to the base of the skull along the side of the neck (Figure 2.2.3). It has mechanical function during head flexion, contralateral (opposite side) axial rotation, and lateral bending. The trapezius runs from the scapula (shoulder blade) and clavicle to the base of the skull and the spinous processes of the thoracic vertebrae forming a triangle. It can cause extension, contralateral rotation, and lateral bending as well as raising the shoulders. The splenius

capitis runs from the spinous processes of the upper three or four thoracic vertebrae to the base of the skull. It has mechanical function in extension, ipsilateral (same side) axial rotation, and lateral bending. The semispinalis capitis connects the upper 6 or 7 thoracic vertebrae and C4-C7 to the base of the skull as well. Most of its length is covered by other muscles especially the splenius capitis. It primarily causes extension.

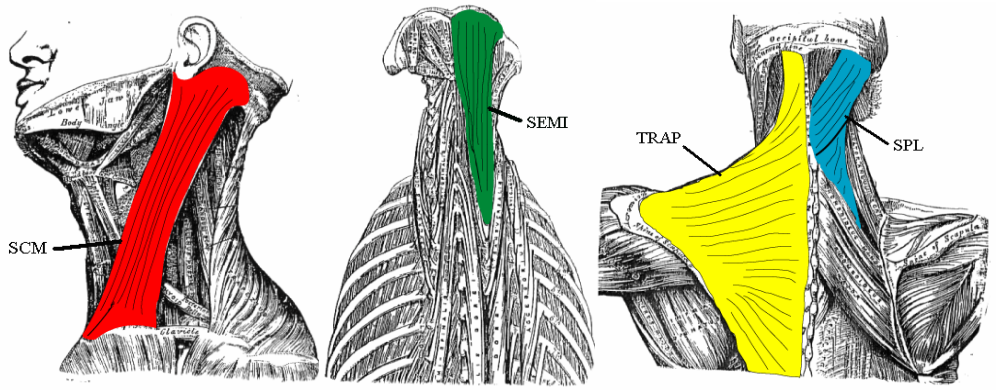

FIGURE 2.2.3 Sternocleidomastoid (SCM), semispinalis capitis (SEMI), trapezius (TRAP), and splenius capitis (SPL) muscle paths in human [6]

2.3 MECHANICAL FUNCTION OF MUSCLES

Muscles are composed of muscle fibers in parallel (Figure 2.3.1). Each fiber is

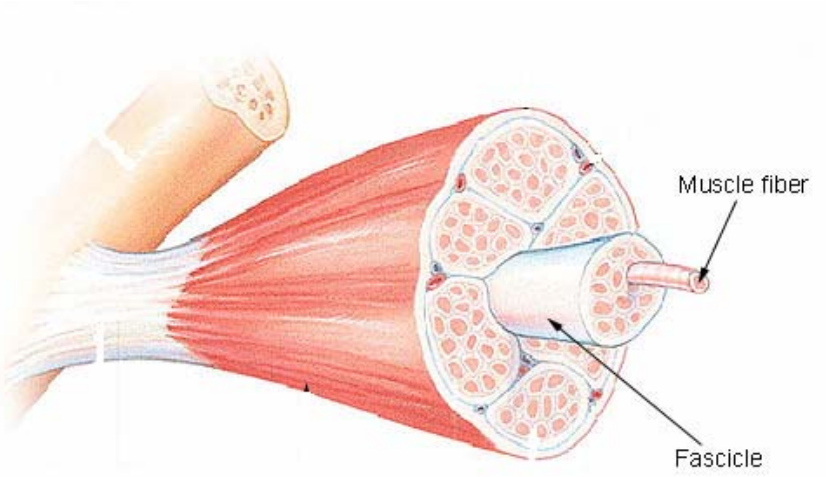

FIGURE 2.3.1 Muscle fibers [8]

composed of myofibrils which are in turn composed of sarcomeres in a repeating pattern (Figure 2.3.2). Each sarcomere contains a staggered arrangement of thick and thin filaments. The thin filaments provide the actin binding sites for the thick filament's myosin heads.

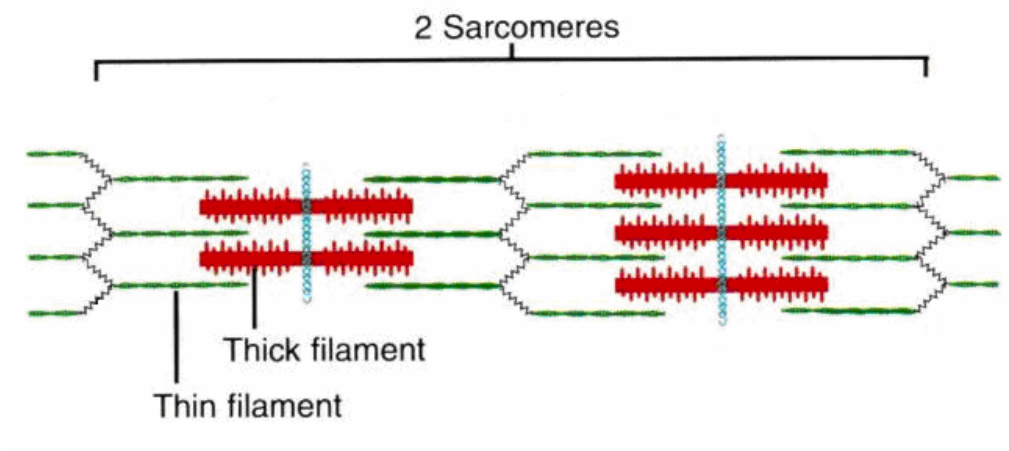

FIGURE 2.3.2 Sarcomere containing thick and thin filaments [9]

Movement is induced by the motor neuron controlling the muscle. It sends an action potential to the muscle, which causes the sarcoplasmic reticulum to release calcium. This calcium binds to the thin filament causing a chain reaction that leaves the actin binding sites on the thin filament free. The myosin heads from the thick filament then bind to these sites forming a crossbridge. Energy is released through the chemical breakdown of ATP (adenosine triphosphate) into ADP (adenosine diphosphate) and Pi (phosphate) causing the myosin head to rotate. If there is nothing to resist motion, this pulls the thin filament past the thick filament (~10nm). If there is an external force resisting shortening, the crossbridge will generate force. The myosin head then releases from the actin binding site and rotates back to its original position. The whole process can then be repeated as long as calcium and ATP are available.

The total force in the muscle is related to the number of crossbridges attached at a particular time. The position of the thick and thin filaments with respect to each other affects the number of usable crossbridges formed in the muscle (Figure 2.4.1). If the thick and thin filaments barely overlap, there are very few crossbridges available and the muscle cannot produce a large force. If they overlap too much, the thin filaments overlap each other which hinder crossbridge forming. The most effective position occurs when all of the myosin heads are within reach of actin binding sites without being obstructed by thin filament overlap. This relationship is called the force-length relationship of skeletal muscles (Figure 2.4.1). It implies that there is a length where the muscle is best suited to supply the most force.

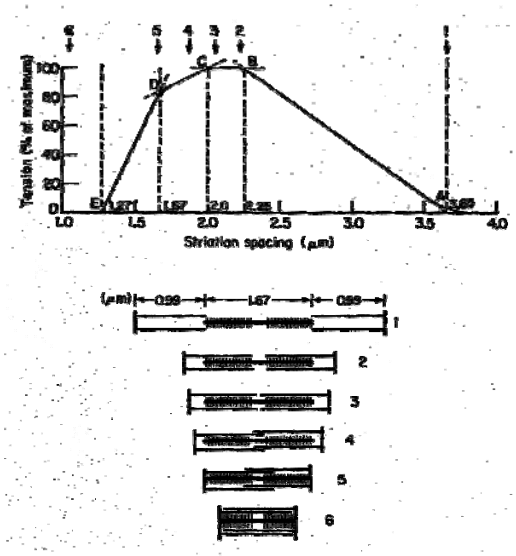

FIGURE 2.4.1 Force-length relationship for skeletal muscles at different filament overlaps [10]

Muscle force is also related to its shortening velocity. For every muscle, there is a maximum shortening velocity which is associated with a no load condition. As the external load increases, the muscle cannot shorten as fast. When the muscle cannot

shorten at all, the magnitude of the load is referred to as the maximum isometric tension. If the load continues to increase, the muscle is forced to lengthen rather than shorten. This relationship is called the force-velocity relationship (Figure 2.4.2). Its implications are that there is a maximum speed of muscle contraction for any given load and that there is an optimum speed for muscle contraction to generate the most power.

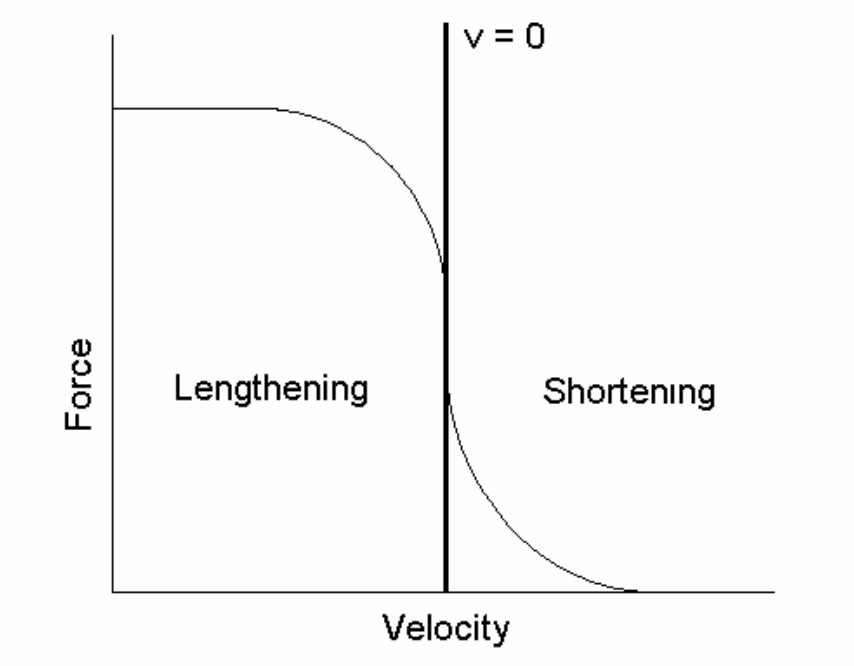

FIGURE 2.4.2 Typical force-velocity relationship for skeletal muscles

2.5 MOMENT ARM

Since skeletal muscles act across joints, the force they generate is transformed to a torque about the joint. The torque which a muscle can produce around a given joint is related to its moment arm, also referred to as a lever arm or mechanical advantage. The muscle's moment arm is defined as the perpendicular distance between a muscle's path and the instantaneous center of rotation of the joint. This distance will change with the position of the joint (Figure 2.5.1). When a muscle spans only one joint, the relationship

between moment arm and angle is relatively easy to determine. However, in systems such as the neck where muscles span multiple joints with motion in more than one plane, the relationship is much more complex since each degree of freedom will have its own associated moment arm.

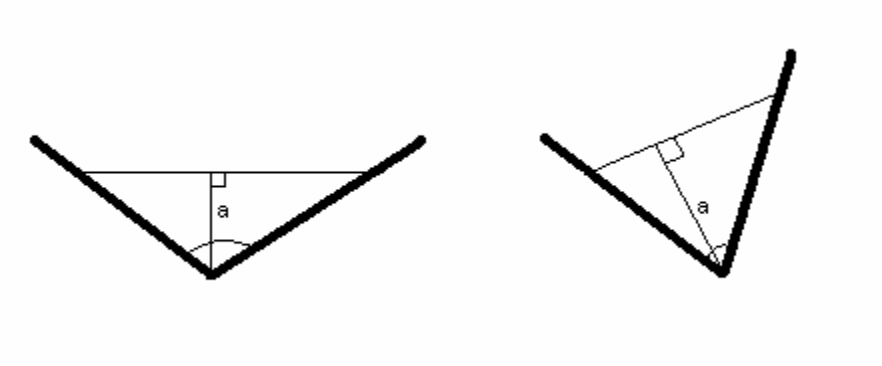

FIGURE 2.5.1 Moment arm (a) changes for joint angle

2.6 REFLEXES

The central nervous system (CNS) uses muscles to stabilize the head in space, as mentioned before. Mechanical signals, such as muscle stretch or head movement, cause a reflex response which leads to activation of muscles. Within skeletal muscles, the muscle spindle generates a reflexive response to muscle stretch (Figure 2.6.1). Muscle spindles lie within the muscle itself. They are composed of intrafusal fibers which lie parallel to the other muscle fibers. Sensory fibers wrap around these and signal neurons in the spinal cord when the muscles are stretched. This causes muscle activation. Therefore, spindles help to increase muscle force and stiffen the muscle if it is subjected to a sudden force. Muscle spindles respond to stretch amplitude and velocity in the muscle.

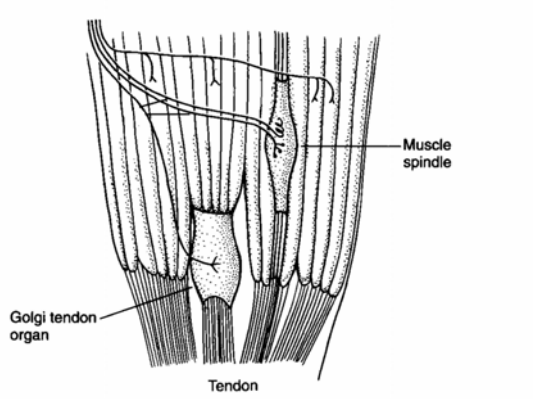

FIGURE 2.6.1 Muscle spindles in a muscle [11] [Kendall, Eric R., Schwartz, James H., Jessell, Thomas M. Principles of Neural Science. Appleton & Lange, Stamford CT (1993). Used by permission of The McGraw-Hill Companies]

The other main reflex, apart from the stretch reflex, involved in stabilizing the head is the vestibular reflex. This reflex is generated in two main areas of the inner ear, the semicircular canals and the otolith organs (the utricule and the saccule) (Figure 2.6.2). The semicircular canals are thought to sense angular acceleration while the otolith organs sense changes in the gravitational force on the inner ear which arise from head linear accelerations. These two work together to keep the head stabilized by sending activation signals to different neck muscles based upon how the head is moving.

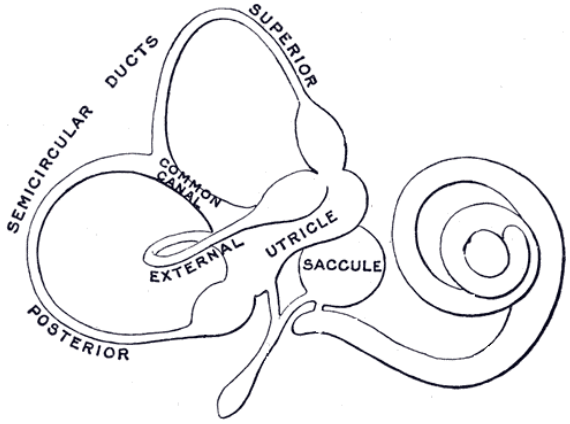

FIGURE 2.6.2 Utricle, saccule, and semicircular canals [6]

There are three semicircular canals in the human body, the superior, posterior, and lateral (Figure 2.6.2). The superior canal is oriented vertically and protrudes from the top of the osseous labyrinth. The lateral canal is also vertical but protrudes from the back of the labyrinth. The posterior canal is oriented in the horizontal plane. Their overall configuration is such that each semicircular canal is at a right angle with the other two like the axes of an orthogonal coordinate system. Thus, each canal is thought to sense motion in a distinct direction.

These two reflexes, the stretch and vestibular, follow different pathways within the nervous system. The vestibular reflex is generated in the inner ear, as mentioned before. The signal then proceeds to the brainstem and from there to the motor neurons of the neck muscles which signal the muscles to react. The stretch reflex, however, is initiated within the stretch receptors in the muscle, as mentioned before. Its signal then travels either directly to the motor neurons for the neck muscles or indirectly through a spinal interneuron to the motor neuron.

2.7 PREVIOUS STUDIES

Other researchers have performed studies to examine the stability and reflex responses of the human head/neck system. Most of them do not push the head directly but rather perturb the body or drop the head. None of these studies mimic our study completely, yet they provide an estimate for our results.

2.7.1 Onset Latencies

Many different studies have looked at the onset latencies in neck muscles during various tasks because it provides an indication of which reflexive pathways were used. These studies used various methods to elicit reflex responses: head drops, release of a weight supported by the head and neck, platform or sled accelerations, or inertial loading to the head.

Ito and colleagues performed two similar studies where the subjects were lying on a table with their heads extending beyond the table and supported by a sling [12, 13]. The sling was then released and the head was allowed to drop. The normal subjects showed an initial burst of activity between 20 and 25 ms and then a larger burst between 40 and 50 ms.

Corna and colleagues [14] performed another study in which the subjects were seated. The subjects were seated and a weight attached to their head was released, applying the force to the head, and the subjects tried to remain in the neutral position. Subjects showed activity at 53 ms in the SPL.

Siegmund and colleagues [15] examined the effects of subject awareness of perturbation magnitude using subjects seated on a linear sled. Three different levels of acceleration were then applied. Their study recorded the SCM and paraspinal (PARA) muscles, a general term representing the extensor muscles in the neck. They measured onset latencies in the SCM of 71 ms for trials in which the subject did not know the force magnitude, unaware, and 68 ms in trials where they did, aware. The PARA muscles had onset latencies of 77 ms in unaware trials and aware trials. There was no statistically significant difference in the neck muscle responses between aware and unaware trials

A second similar study by Siegmund and colleagues [16] used the same setup to investigate the effects of perturbation timing on the subject's response. They found SCM and PARA onset latencies at around 70 and 75 ms, respectively, for all conditions. They found only slight changes between aware and unaware subjects.

Blouin and colleagues [17] did a study where the subjects were seated on a linear sled similar to Siegmund's studies but with two conditions, the subjects initiated the forward translation themselves (predictive) or a verbal signal was given and 0.5-5 seconds later the translation occurred (reactive). Their onset latencies in the reactive trials were 52 ms for the scalenus and 54 for the SCM. The latencies in the predictive trials were lower, 45 and 46 ms respectively. Unlike in Siegmund's study, they found less muscle activity and shorter onset latencies in the in the predictive case than the reactive case. This hints at a different response when subjects are aware of the oncoming perturbation.

Kuramochi and colleagues [18] did a study in which seated subjects were hit on the forehead by a pendulum with either their eyes open (EO) or eyes closed (EC). They recorded onset latencies of around 20 ms in the SCM in the EC condition. The investigators also found that the SCM responses were significantly smaller in the EO case than the EC case. This again seems to suggest that knowledge of the impending perturbation changes the subjects' responses

Horak and colleagues performed a study [19] in which the subjects wore a backpack device which applied perturbations to the subjects' heads. In forward head translation trials, normal subjects showed a burst in both the TRAP and SCM at 51 ms. In the backward head translations, the normal subjects showed bursts in the TRAP at 48

ms and at 71 ms in the SCM. Schupert and Horak performed a similar study later [20] in which the platform went back and forth while the subjects wore the backpack device. The normal subjects showed responses in both muscles at around 50 ms in forward head perturbation trials.

Tierney et al. [21] performed a study in which forces were applied directly to the head via a dropped weight. They found the average onset latencies in the SCM and TRAP at around 45 ms for males and 35 ms for females. Mansell et al. [22] used the same force applicator to perform a study which focused on the effects of training on head/neck reflex responses. They found TRAP onset latencies around 30 ms for men and 22 ms for women. The SCM activated at around 42 ms for males and 24 ms for females.

Our study is designed to be most similar to the Kuramochi, Horak, Tierney, and Mansell studies in that we will apply forces directly to the subjects' head. Because of this, we expect our onset latencies to be most similar to these and range between 20 and 70 ms.

Several studies looked at the difference between normal subjects and labyrinthine-defective patients' responses [12, 13, 14, 19, 20, 23]. Labyrinthine-defective patients are people who have lost their vestibular function and thus rely on different mechanisms to control their head's position in space than normal subjects. By comparing the responses of these two groups, investigators can learn the effect the vestibular reflex has on the response to head perturbations. In most of these studies, the labyrinthine-defective patients showed delayed or no responses to forced head translations. However, the Horak and Schupert studies [19, 20] looked at two types of vestibular loss patients, ones who had lost function during childhood and ones who had during adulthood. Interestingly, in

both of these studies at least one of the childhood loss patients showed an earlier than normal onset latency for some of their EMG's. This suggests that the CNS is able to adapt to setbacks like vestibular loss given enough time.

Mazzini and Schieppati calculated the voluntary reaction times for subjects' head/neck systems. They were all between 103 and 118 ms for the SCM and SPL on both sides [24]. This provides a cut-off time for reflexive onset latencies.

2.7.2 Stiffness and Damping Coefficient

Very few studies have quantified the stiffness of the human head/neck system. Fard and colleagues [1] performed a study where they seated male subjects on a horizontal vibration table, strapped their torso in, and applied a random vibration in the front to back direction. They modeled the head-neck complex as a double-jointed inverted pendulum and calculated the stiffness and damping coefficient of the two joints, the head and neck, based upon the positional data. Their neck stiffness was 15.57 Nm/rad and the damping coefficient was 0.358 Nms/rad. Their head stiffness was 10.45 Nm/rad and the damping coefficient was 0.266 Nms/rad.

Tierney et al. and Mansell et al. [21, 22] also determined the head-neck segment stiffness for their subjects. They defined their stiffness as the slope of the change in force versus the change in angular position during the first cycle following the perturbation. As such, their stiffness values were not determined by modeling the system as an inverted pendulum and are in units of lbf/°. Their values do provide a rough reference for the stiffness though. In the Tierney study, two cases were studied, one where the timing of the perturbation was known and one where it was not. Their results were divided by sex and direction (flexion and extension) as well as known and unknown timing (Table

2.7.1). Only physically active subjects were used. They found that males were generally stiffer than females and that males responded differently to perturbations where the timing was known versus unknown but females did not.

TABLE 2.7.1 Stiffness results, average ± standard deviation, from Tierney's study [21]

Gender	Knowledge	Direction	Stiffness (lbf/°)
Male	Known	Flexion	1.29 ± 0.39
		Extension	1.75 ± 0.55
	Unknown	Flexion	1.34 ± 0.66
		Extension	1.26 ± 0.40
Female	Known	Flexion	0.92 ± 0.43
		Extension	1.21 ± 0.55
	Unknown	Flexion	0.88 ± 0.47
		Extension	1.00 ± 0.48

Mansell et al.'s study [22] used collegiate soccer players. It focused more on the effects of a neck strengthening regimen for female athletes versus male athletes and only looked at flexion. Their stiffness was obtained in the same manner and is shown below (Table 2.7.2). They did not find a difference in the stiffness between males and females.

TABLE 2.7.2 Stiffness from Mansell's study [22]

Gender	Knowledge	Stiffness (lbf/°)
Male	Known	0.84
	Unknown	0.81
Female	Known	0.88
	Unknown	0.58

These are the only known values to compare with our results. Two studies done by Keshner and colleagues [25, 26] compared horizontal rotation (yaw) with vertical

rotation (pitch). They concluded the stiffness in pitch may be larger than in yaw but did not calculate these values.

2.8 SYSTEM IDENTIFICATION

Previous studies have modeled the human head/neck system as an inverted pendulum (Figure 2.8.1), a second order, rotational system [1, 2, 3]. The studies concluded that their models fit the data well. The stiffness and damping coefficient of the system are obtained using system identification.

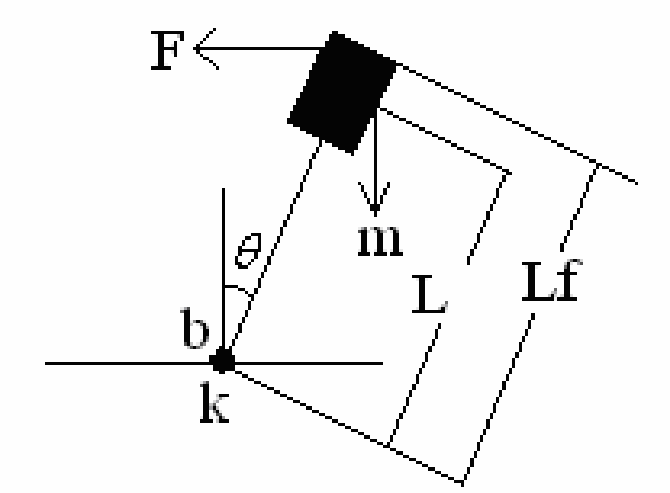

FIGURE 2.8.1 Inverted pendulum with spring and damping

The derivation of the basic equation of motion for this inverted pendulum begins with a simple sum of the moments (Equation 1).

$$\sum M = I\ddot{\theta} \tag{1}$$

In this equation, M is the moments, I is total moment of inertia for the system, and $\ddot{\theta}$ is the resulting angular acceleration of the system. By applying this to the system shown in figure 2.8.1 and defining θ as positive to the right, equation 1 becomes

$$I\ddot{\theta} = FL_f - B\dot{\theta} - K\theta + mLg\sin\theta \quad (2)$$

where F is the applied force, L_f is the moment arm of the applied force, B is the rotational damping coefficient, K is the rotational stiffness, m is the mass of the system, L is the length to the center of mass, g is the gravitational constant, $\dot{\theta}$ is the angular velocity, and θ is the angular position. F, $\ddot{\theta}$, $\dot{\theta}$, and θ are all functions of time. K, B, m, L, g, and L_f are constants.

If the force is applied for a short period, as in these experiments, and the evaluation starts after the force is applied, then the force will equal 0. Equation 2 then becomes

$$I\ddot{\theta} + B\dot{\theta} + K\theta - mLg\sin\theta = 0 \quad (3)$$

with small angle assumptions ($\sin\theta = \theta$) equation 3 becomes

$$I\ddot{\theta} + B\dot{\theta} + (K - mgL)\theta = 0 \quad (4)$$

This equation is easier to deal with if the K-mgL term is replaced as follows

$$\kappa = K - mgL \quad (5)$$

Then equation 4 becomes

$$I\ddot{\theta} + B\dot{\theta} + \kappa\theta = 0 \quad (6)$$

This equation is solved using differential equations. The basic solution for equation 6 is

$$\theta(t) = c_1 e^{r_1 t} + c_2 e^{r_2 t} \quad (7)$$

where c_1 and c_2 are constants determined by the initial conditions, r_1 and r_2 are the roots of the characteristic equation, and t is the time.

Solving for the constants and simplifying equation 7 leads to

$$\theta(t) = Ae^{-\zeta\omega_n t}\sin(\omega_d t + \phi) \tag{8}$$

where A (amplitude) and ϕ (phase) are constants that are determined through boundary conditions. ζ is the damping ratio, ω_n is the frequency of oscillation, and ω_d is the damped natural frequency. They are defined as

$$\zeta = \frac{B}{2\sqrt{I\kappa}} \tag{9}$$

$$\omega_n = \sqrt{\frac{\kappa}{I}} \tag{10}$$

$$\omega_d = \omega_n\sqrt{1-\zeta^2} \tag{11}$$

By minimizing the sum of the squares of the error between equation 8 and the experimental data, $(\theta\text{-data})^2$, optimized values of K and B are obtained for a given system. This method is particularly useful when only positional data are available for the experiment, as in the following experiments, since the derivative of the data is not needed for the fit.

CHAPTER THREE

DEVICE DESIGN

The first phase of this project involved designing and building a device with which we could perform our experiments. A previous device had been built using the current motor to pull on the subjects' head in various directions. This device needed to be evaluated to determine if a new one was necessary. This evaluation led to the conclusion that an entirely new frame was necessary. Additional components (linear screw drive, load cell) were incorporated into the new frame. The motion analysis system, accelerometers, and electromyography equipment used in the experiments are also described below.

3.1 OLD FRAME

The previous device was a simple, wooden construction (Figure 3.1.1) attached to a dental chair. Eight cables ran in different directions (0°, 45°, 90°, 135°…) through pulleys to the motor on a table behind the setup. These cables allowed the motor to pull the subject's head in any of the 8 directions.

FIGURE 3.1.1 Old frame

The frame had many different problems. The more crucial problems were as follows:

1. The cables had too much slack in them which led to both a long delay between the motor firing and the helmet being pulled and a negligible movement of the helmet.
2. The frame could not be raised high enough to accommodate a tall person.
3. The entire cable system had large amounts of friction.
4. The frame shook when the motor was fired.
5. When one cable was pulled, the helmet moved in all directions, not just the desired one.

3.2 NEW FRAME

After evaluating the old frame, we decided to build a new frame which pushed the head rather than pulled it. When designing the current device, we came up with five goals for the device.

1. Apply forces in the horizontal plane to a subject's head while isolating it from the torso
2. Apply the forces in any direction in the horizontal plane
3. Allow for subjects between 5'3" and 6'4" tall
4. Be completely safe to the subject
5. Frame's motion does not interfere with the experiments.

The new frame (Figure 3.2.1) is free standing with the dental chair placed underneath. It is built from Bosch Rexroth tubing, 30 x 30 mm. The frame is made up of front and back supports with a suspended section between the two. The rear support is two columns spaced about 18 cm apart with horizontal bars running between them. The front support is a long beam supported at both ends. The suspended section attaches to the center of the front support and to the top of the rear supports. It is made of two beams spaced the same as the rear support. For more support, two horizontal beams across the front of the frame and two diagonal beams from either end of the front section to the back were added. Cables anchoring the frame to the wall were also added for extra support. The frame is roughly 200 cm tall, 170 cm wide, and 105 cm deep.

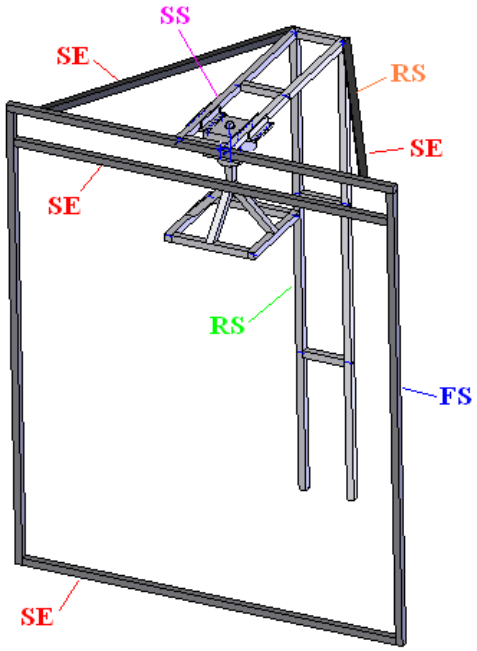

FIGURE 3.2.1 New frame with rear support (RS), front support (FS), suspended section (SS), and stabilizing elements (SE) shown

Two sliding mechanisms, also from Bosch, are attached to the suspended section. The motor mount hangs from the rotator which is attached to these sliders (Figure 3.2.2). The rotator (Figure 3.2.2) consists of a large block of aluminum with a hole in it. A

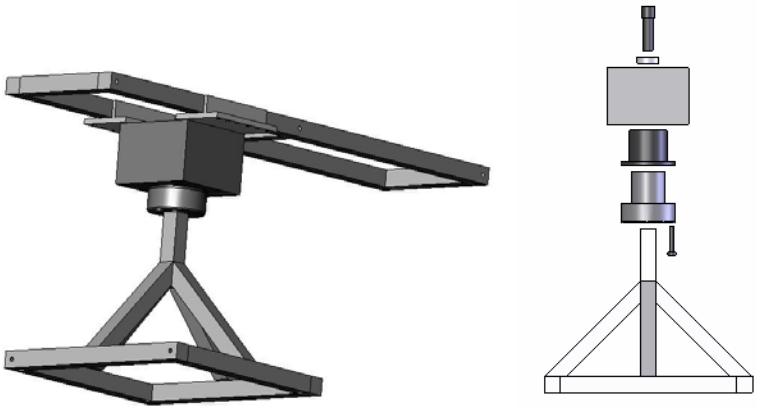

FIGURE 3.2.2 Rotator attached to sliders (left) and expanded view of rotator (right)

sleeve of delrin goes inside this hole and a mushroom-shaped piece of aluminum goes inside of this, with the stem slipping into the sleeve. The motor mount attaches to the cap of the mushroom-shaped piece. A locking bolt is in the top of the mushroom-shaped piece. A circular pattern of holes was drilled in the aluminum block (Figure 3.2.3) so that by inserting the locking bolt into them, the motor mount is fixed at different angles from the frame. Increments of 45° were chosen initially, but any angle could be drilled in the future.

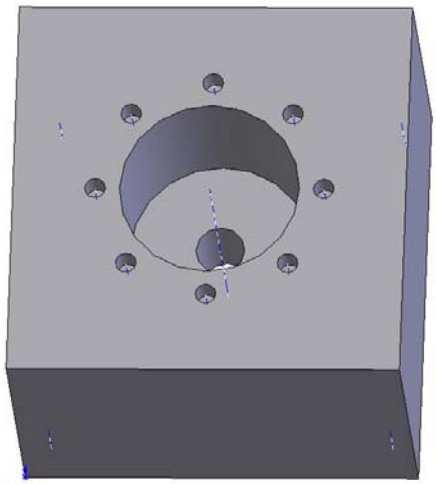

FIGURE 3.2.3 Circular pattern of holes in aluminum block of rotator

The motor mount (Figure 3.2.4) has four bars hanging diagonally down from the rotator to a square frame such that it resembles a pyramid. A linear screw drive (Velmex MB2515W4J-S2.5, Bloomfield, NY) is attached to the bottom of the square frame. This applies the perturbation to the subject's head.

Stops were added as well (Figure 3.2.4) to stop the subject from moving too far and possibly injuring themselves. They are seen in the left hand side of the figure hanging from the motor mount and reaching below the linear screw drive.

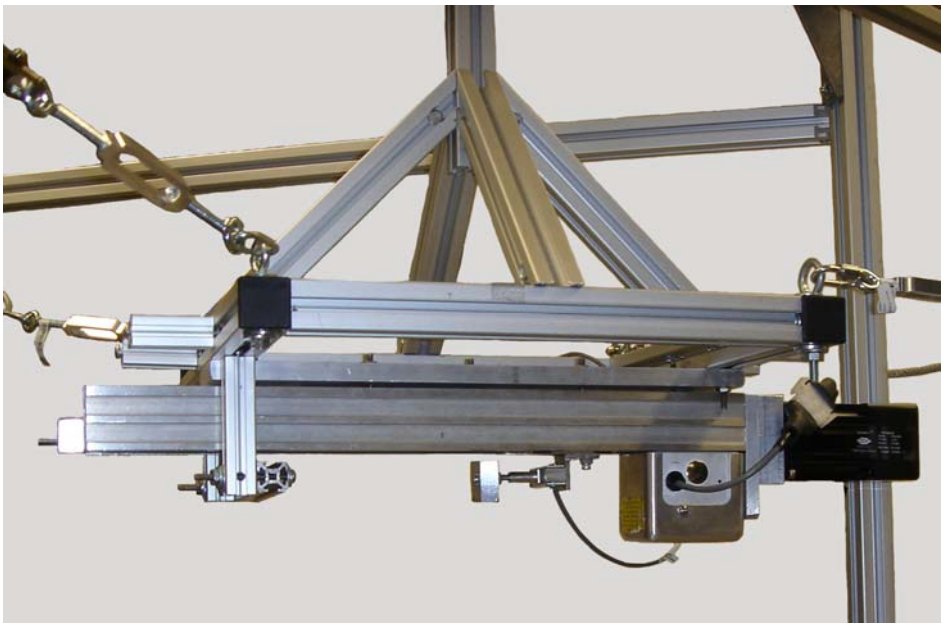

FIGURE 3.2.4 Motor mount of new frame showing linear screw drive and stops

The subject will sit in a modified dental chair. Safety belts will hold the subject in place during the test. The subject will wear a replacement frame for a welding helmet with a bolt sticking up from the top (Figure 3.2.5). Perturbations are applied to a block of wood attached to the top of the bolt. Sheet metal reinforces the strap that goes over the top of the head. This should allow for a better force transfer from the spike to the head. The helmet's mass is low (223 grams) and should add little to the moment of inertia of the subject's head.

FIGURE 3.2.5 Helmet for human subject experiments

3.3 MOTOR ASSEMBLY

The motor used is a SmartMotor 2330D (Animatics SM2330D, Santa Clara, CA). This motor is controlled via the computer using the SmartMotor Interface (SMI) software. We can use it in two different modes, torque mode and position mode. As the name suggests, position mode controls the position, acceleration, and maximum velocity for the motor's motion. Torque mode actually controls the power output of the motor rather than the torque. Since Power = Torque*Velocity, if the velocity is varying then the torque will vary as well (Figure 3.3.1). However, there is a range of velocity up to about 500 rpm where there is no torque change. For our experiments, we used the torque mode since it resulted in a more consistent output force.

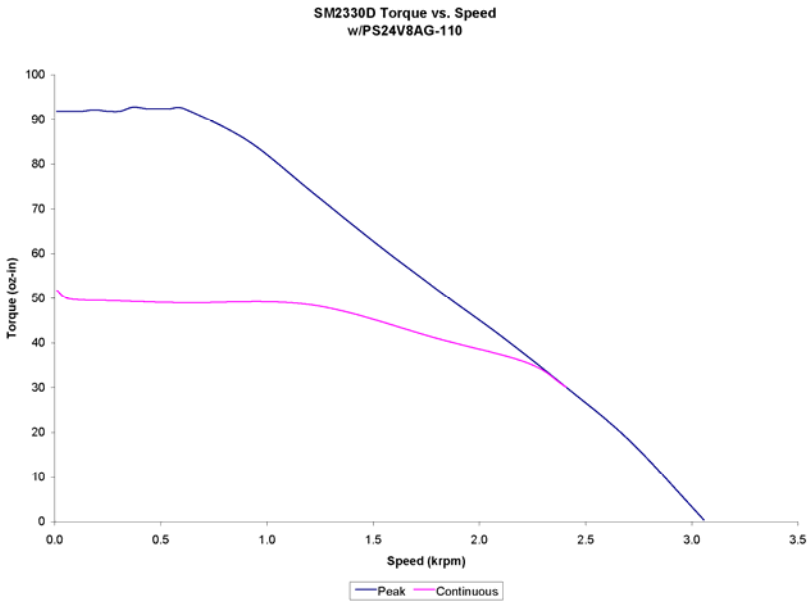

FIGURE 3.3.1 Torque velocity relationship for motor

The motor is attached to a linear screw drive with a pitch of 0.4 in. The linear screw drive converts the motor's rotational motion into linear motion by using the motor to turn a screw. A sled is mounted on the screw and advances or retreats with the screw's motion. Variable limit switches are built into the screw drive. If the sled moves too far, the switch is activated and the circuit is cut. The switches are wired in line with the power supply to the motor. Thus, the sled moving too far causes the motor to lose its power supply. This is one of the safety devices in the setup. The other is a master kill switch which the subject will hold. The subject can push this switch before or after the motor begins to move and stop the motor from moving forward.

We attached a load cell (Omega LC703-10, Bridgeport, NJ) via an L-bracket (Figure 3.3.2) to the sled on the screw drive. A small aluminum block is connected to the load cell via a bolt. This block applies the force from the motor. The force is thus

applied via the load cell, allowing the force to be measured. The load cell supplies a continuous signal and is attached to a 10 kHz bandwidth signal processor (Omega OM5-WBS, Bridgeport NJ). This output is then sent to the OptoTrak Data Acquisition Unit (ODAU, see OptoTrak section) where it is recorded.

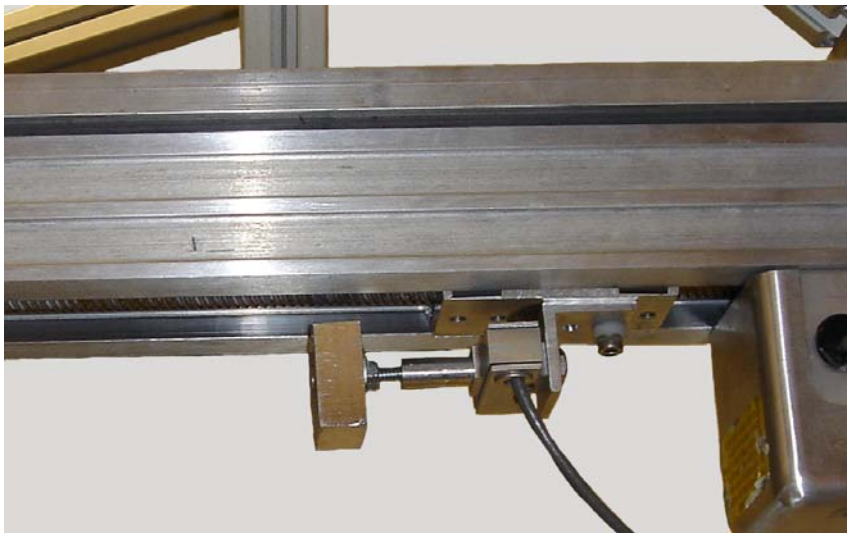

FIGURE 3.3.2 Load cell attached to linear screw drive

3.4 POSITIONING SYSTEM

As mentioned before, we used an OptoTrak (Northern Digital OptoTrak 3020, Waterloo, Ontario Canada) opto-electronic motion analysis system to record the position in our experiments with a minimum inaccuracy of 0.005%. The system consists of three components, the system control unit (SCU), the cameras, and the ODAU. The cameras and ODAU connect to the SCU which in turn connects to the computer. Three cameras record the three-dimensional position of infra-red emitting markers in a coordinate system defined by the cameras. These markers are placed on the object of which you wish to record the position. The ODAU allows the OptoTrak to record analog voltage signals from different devices. We used this to record the accelerometer outputs,

electromyograph signals, and load cell signal during the experiments. The NDI Toolbench software allows the user to view and manipulate the inputs from both the cameras and the ODAU before they are recorded in data files.

To define the head kinematics, we used the rigid body feature of Toolbench. With this feature three or more markers are grouped together and treated as a solid object. The markers must be perfectly rigid with respect to each other and at least three markers within the rigid body must be visible to the cameras at all times. The 3D rotations and translations of the rigid bodies in the OptoTrak's coordinate system are recorded and saved in a data file. The OptoTrak defines the x axis as pointing up, the y axis as pointing to the left when looking away from the OptoTrak, and the z axis as towards the OptoTrak.

3.5 ACCELEROMETERS

We used dual-axis accelerometers (Analog Devices ADXL210, Norwood MA) for the experiments. These accelerometers had a range of ±10 g. The signal from the accelerometers was routed into the ODAU. The accelerometers required a 5 volt power supply which we provided by running the accelerometers in parallel from the same supply.

3.6 ELECTROMYOGRAPHY

Electromyographs (EMG) measure the activation of muscles. They do this by measuring the electrical potential (electromyogram) in the muscles. As mentioned

before, action potentials propagate within the muscle to activate the muscles. As these propagate, a current flow is generated. The EMG measures the potential between two points on the muscles, thus measuring the activation in the muscles. This potential is compared with a reference electrode placed somewhere above bone, for example the knee or elbow.

The EMG electrodes we used (Delsys Bagnoli 8 System, Boston MA) are differential surface electrodes meaning they are placed on the skin above the muscle and use two contacts to measure the potential. The contacts are made of silver and are 10 mm apart. The Delsys system provides amplification to the EMG signals at different levels (100, 1,000, and 10,000).

3.7 FRAME STIFFNESS

The frame was tested to determine that its motion does not interfere with the experiments. Knowing the approximate motion of the force applicator, we decided that if the frame's motion was two orders of magnitude less than the motion of the force applicator the frame's motion would not interfere with the experiments.

After initial testing, cables were added to anchor the frame to the wall. These were placed on the frame on the top, front, right and left corners and the top, rear, left corner (Figure 3.3.3). The frame was tested again and more cables anchoring the motor mount to the rest of the frame were added (Figure 3.3.3).

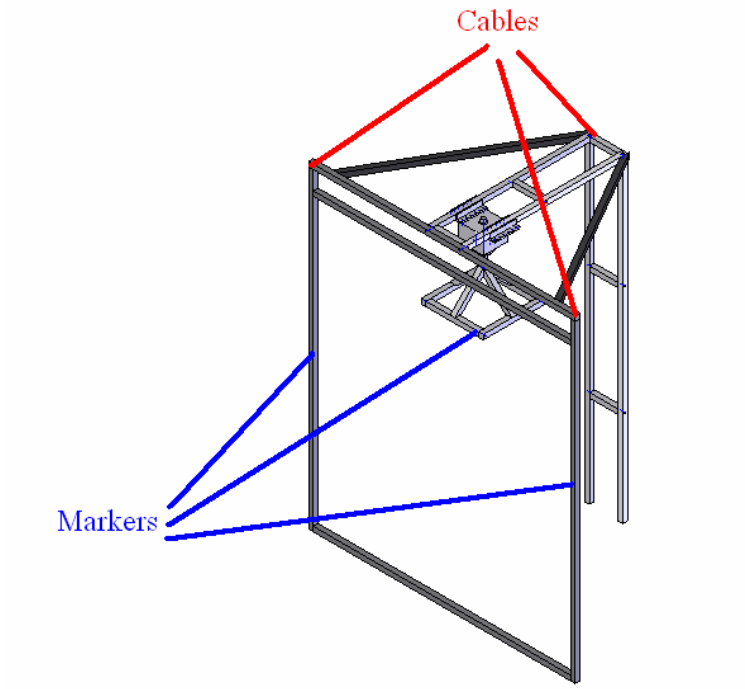

FIGURE 3.3.3 Cable and marker positions on frame

After the motor mount cables were added, markers were placed on the frame (Figure 3.3.3) and trial runs for human subject experiments were performed. The marker on the motor mount averaged 0.20 mm of motion at most. The marker on the front right of the frame (referenced as looking at the frame) averaged 0.05 mm of motion at most. Finally, the marker on the front left of the frame average 0.98 mm of motion at the most. These motions were two orders of magnitude less than the force applicator's motion, 48 mm during the trials. The frame's motion was thus deemed not to interfere with the experiments.

CHAPTER FOUR

INVERTED PENDULUM EXPERIMENT

4.1 INVERTED PENDULUM METHODS

The second part of the experiment was to use the new device to test a known system. Since the head/neck system is often modeled as an inverted pendulum [1, 2, 3], we built an inverted pendulum to test. By performing similar tests on the inverted pendulum as we will perform on the human subjects, we can refine our methods for testing a system (applying a force, measuring motion, and curve fitting to calculate the stiffness and damping parameters).

4.1.1 System

The neck was represented by a hollow aluminum tube (Figure 4.1.1). A hole was drilled through the bottom of the neck and an axle was put through it. The head was represented by a hollow steel tube which fit over the neck. Three holes were drilled in the bottom of the head and the top of the neck at 90° to each other (0°, 90°, and 180°). Locking screws were screwed into these holes to hold the head and neck together.

FIGURE 4.1.1 Drawing of inverted pendulum

The axle was mounted in four bearings, two per side. The bearings were mounted to a steel plate using L-brackets (Figure 4.1.2). On the other side of the steel plate, an aluminum plate was mounted vertically using L-brackets. Two bolts held a spring between the plate and the neck.

FIGURE 4.1.2 Picture of entire inverted pendulum setup

4.1.2 Spring Constant

Although we were testing a rotational system, the spring was a linear rather than rotational spring. Slight changes in the spring's path occurred during testing which could lead to non-linearities in the model. For small angular motions, we assumed linearity in the model. The manufacturer did not supply a spring constant so this was determined first. To do this, the spring was hung from a hook. Masses were hung from the spring and the length change was recorded. The mass values were used to obtain the forces.

The length changes were graphed for the different forces and a linear regression fit was used to determine the spring's stiffness of 1346 N/m.

4.1.3 Testing

The inverted pendulum was placed under the frame and secured in place so that the motor applied a force to the top of the head. A rectangular piece of aluminum hung from the head provided a place to attach four positional markers. A second piece of aluminum was attached to the base to provide a location for four markers making a coordinate system. The OptoTrak system recorded the position of these four markers during the tests. The motor was programmed to apply a force and then immediately move out of the way to allow the system to respond naturally. We ran 20 tests for three different motor programs which were designed to give three different forces averaging 3.9 N, 6.8 N, and 9.6 N.

4.1.4 Analysis

The equation of motion for our system is derived by performing a moment analysis (Figure 4.1.3).

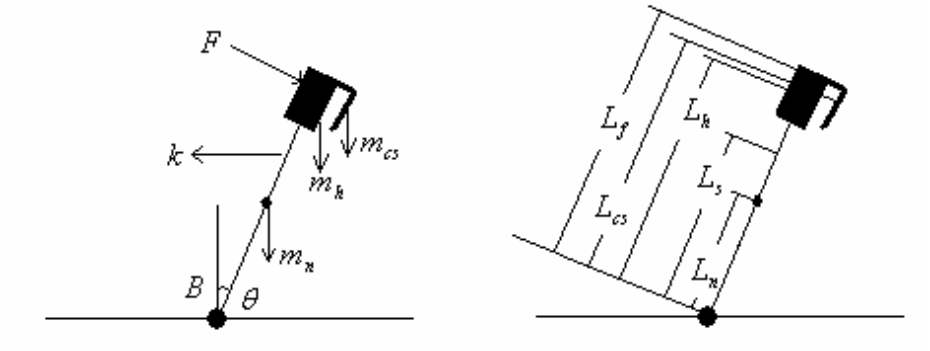

FIGURE 4.1.3 Sum of the moments for the inverted pendulum

Summing the moments in this figure yields

$$I\ddot{\theta} = (m_n L_n + m_h L_h + m_{cs} L_{cs})g \sin\theta + FL_f - kL_s^{\,2} \sin\theta\cos\theta - B\dot{\theta} \qquad (12)$$

In equation 12, B is the rotational damping coefficient, k is the linear spring constant, I is the total moment of inertia about the rotation axis, F is the force applied as a function of time, θ is the angle, $\dot{\theta}$ is the angular velocity, $\ddot{\theta}$ is the angular acceleration, and g is the gravitational constant. The mass and lengths to the center of mass of the different segments are denoted by m and L. The subscripts n, h, and cs refer to the neck, head, and aluminum piece hanging from the head respectively (Table 4.1.3). All the lengths are measured from the center of rotation of the system.

TABLE 4.1.3 Various constants for the inverted pendulum

Variable	Value
L_s (m)	0.2328
L_n (m)	0.1471
L_h (m)	0.3238
L_cs (m)	0.3362
I_h (kg m^2	0.5473
I_n (kg m^2)	0.0101
I_cs (kg m^2)	0.0119
I_tot (kg m^2)	0.5693

Applying the small angle assumption ($\sin\theta \approx \theta$ and $\cos\theta \approx 1$) and ignoring the force (see System Identification) yields

$$I\ddot{\theta} + B\dot{\theta} + [kL_s^{\,2} - (m_n L_n + m_h L_h + m_{cs} L_{cs})g]\theta = 0 \qquad (13)$$

Comparing equation 13 with equation 6 in the system identification section (Section 2.8) shows that

$$\kappa = kL_s^2 - (m_n L_n + m_h L_h + m_{cs} L_{cs})g \qquad (14)$$

This is solved using the same methods described in the system identification section. The boundary conditions are

$$\theta(0) = \theta_0 = A\sin\phi$$
$$\dot{\theta}(0) = 0 = -\zeta\omega_n A\sin\phi + A\omega_d\cos\phi \quad (15)$$

Solving for A and ϕ leads to

$$A = \frac{\theta_0}{\sin\phi} \quad (16)$$

$$\phi = \cos^{-1}\zeta \quad (17)$$

Equations 16 and 17 were plugged into the general solution in the system identification section (Equation 8) to solve for the k and B of the system by minimizing the sum of the square of the errors.

4.1.5 Statistical Analysis

Analysis of variance was performed on the stiffness and damping coefficient of the system to determine whether the results calculated from applied different force values were statistically different.

4.2 INVERTED PENDULUM RESULTS

Our determined stiffness and damping coefficient were consistent and accurate (Table 4.2.1). The overall average of the resulting stiffness (k) was 6% higher than the measured (1427.1 N/m and 1346.1 N/m respectively). We could not directly measure the damping coefficient to compare our results with but our results were consistent across all

force levels (0.12 ± 0.01 Nms/rad overall). Comparing the curve fit with the actual data led to R^2 values of over .9 for every trial (Figure 4.2.1).

TABLE 4.2.1 Average and standard deviation of force (F), stiffness (k), damping coefficient (B), and R^2 for tests

Force	Low	Medium	High	Overall
F (N)	3.90 ± 0.04	6.79 ± 0.04	9.56 ± 0.04	
k (N/m)	1449.5 ± 4.5	1427.1 ± 0.9	1404.7 ± 3.4	1427.1 ± 18.7
B (Nms/rad)	0.13 ±0.02	0.13 ± 0.00	0.10 ±0.00	0.12 ± 0.01
R^2	0.96 ± 0.02	0.95 ± 0.00	0.99 ± 0.00	0.97 ± 0.02

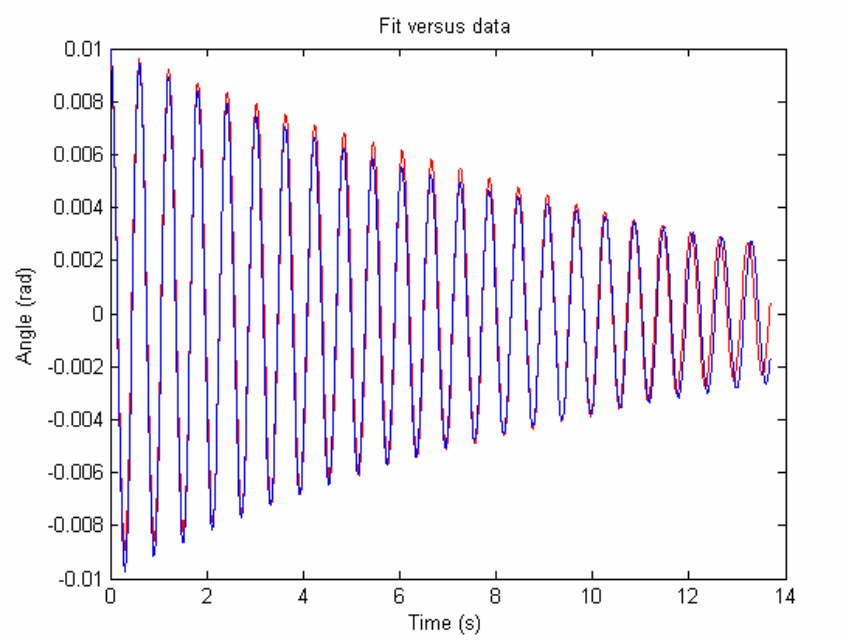

FIGURE 4.2.1 Representative graph of curve fit (blue) versus data (red)

The values for the stiffness decreased with increasing load (Figure 4.2.2 and Table 4.2.1). According to an ANOVA test on all three force levels, at least one of the means of the k's for the three forces was different (p<0.05). Post-hoc t-tests between the pairs of forces showed that all 3 means were significantly different.

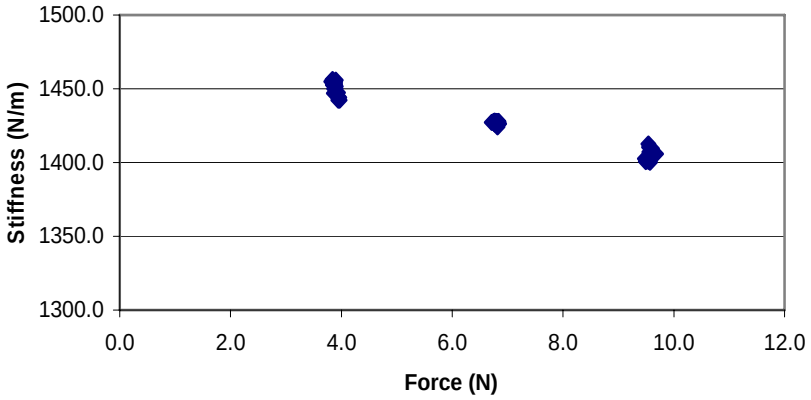

FIGURE 4.2.2 Force versus stiffness

Unlike the stiffness, the damping coefficient was consistent across force levels (Figure 4.2.3 and Table 4.2.1). It is interesting to note that B was grouped for the high and medium forces, but it was less consistent for the low forces. The overall standard deviation of 0.01 was less than 15% of the average (0.12). According to an ANOVA test, at least one mean was different from the others across the three force levels (p<0.01). T-tests between the various pairs showed that only the low and medium force levels have means that may be significantly different (p = .05).

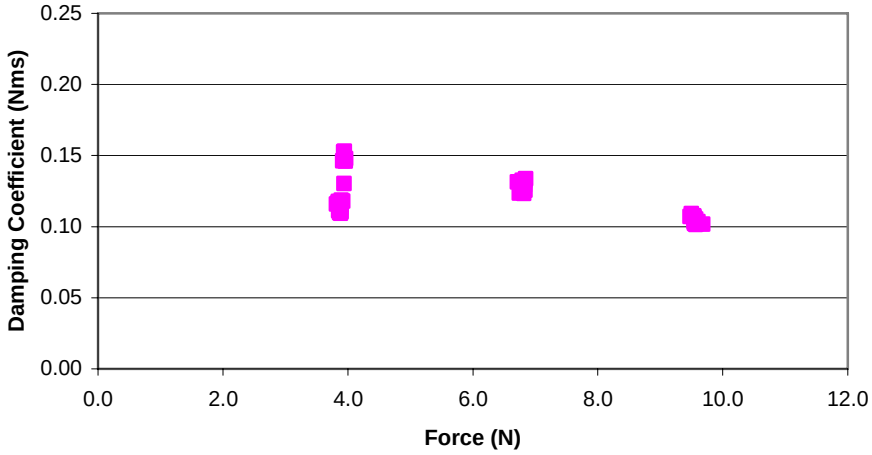

FIGURE 4.2.3 Force versus B

The R^2 values were over 0.9 for every trial, indicating good fits model and data. The low and medium forces had lower R^2 values, while every high force trial had an R^2 value over 0.99, showing very good fits.

4.3 INVERTED PENDULUM DISCUSSION

There are a number of different explanations for the error in our stiffness estimation. The spring in the inverted pendulum did not have a straight path; it bent slightly (Figure 4.3.1). It is also very likely that the spring was either compressed or stretched at the beginning of the trials. This initial stretch or compression would balance the initial torque due to the weight of the pendulum which would occur if the pendulum was not perfectly vertical. However, by defining the initial angle as 0 rad, these two initial forces are ignored in the curve fit since they are constants which cancel each other. A range of initial stretch/compression (more than 2 times the maximum motion of the pendulum) was accounted for while measuring the stiffness of the spring by using a larger range of forces than were applied in the trials.

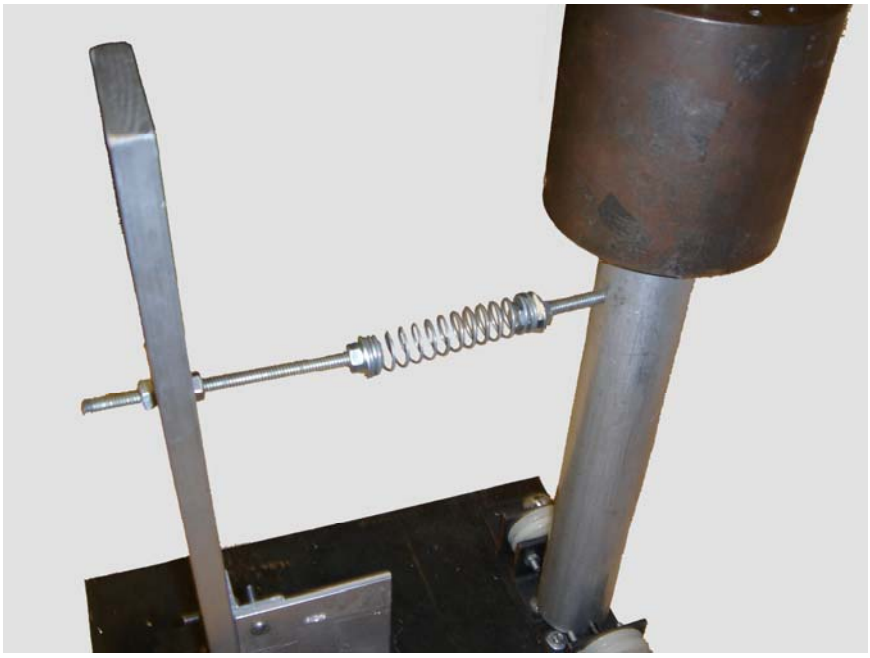

FIGURE 4.3.1 Setup showing path of spring

The consistency of the damping coefficient leads us to believe that it is accurate for our system. We cannot measure the damping coefficient directly. However, if the peaks of the angle data are fit with an exponential, the B is obtained from the logarithmic decrement as shown below (Equations 18-22).

$$Peaks = e^{-\zeta\omega_n t} = e^{-ct} \tag{18}$$

$$B = 2\zeta\sqrt{IK} \tag{19}$$

$$K = I\omega_n^2 \tag{20}$$

$$B = 2\zeta\sqrt{II\omega_n^2} = 2I\omega_n\zeta \tag{21}$$

$$B = 2Ic \tag{22}$$

Our results from fitting all the data produced an average B of 0.12 Nms/rad. The logarithmic decrement method determined an average B of 0.11 Nms/rad. The logarithmic decrement is essentially the same as our curve fit method. However, by

comparing the two methods, we can check that our curve fit is finding the overall minimum for the sum of the squares of the errors and not just a local minimum.

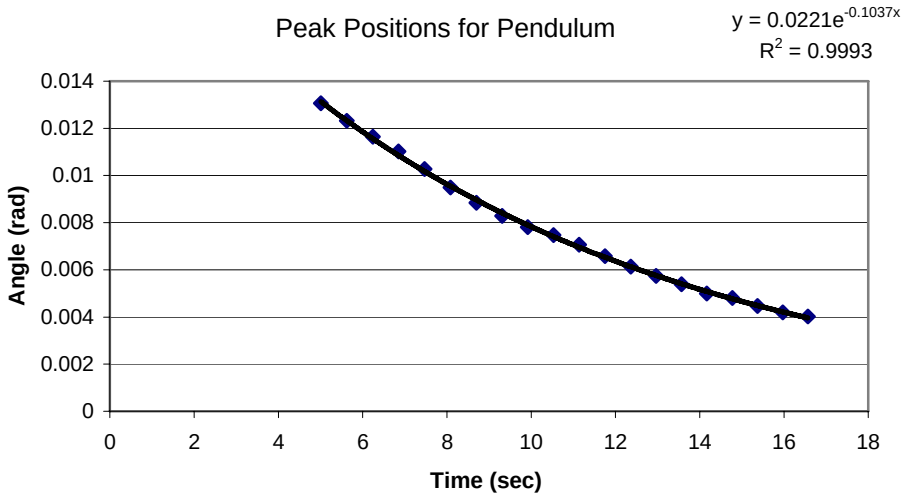

FIGURE 4.3.2 Curve fit for peak amplitudes to obtain B

The constants used in the parameter estimation had a large impact on the determined stiffness of the system. Increasing the inertia of the system by 10% led to an 8% increase in the estimated stiffness and 10% increase in estimated damping coefficient. Although the measurements for these parameters were repeated several times, there may have still been minimal error. Any error would affect the stiffness estimated by the curve fit.

It is also interesting to note that the errors in the curve fit occurred when the motion of the pendulum was small (Figure 4.3.3). The largest motion seen in these trials

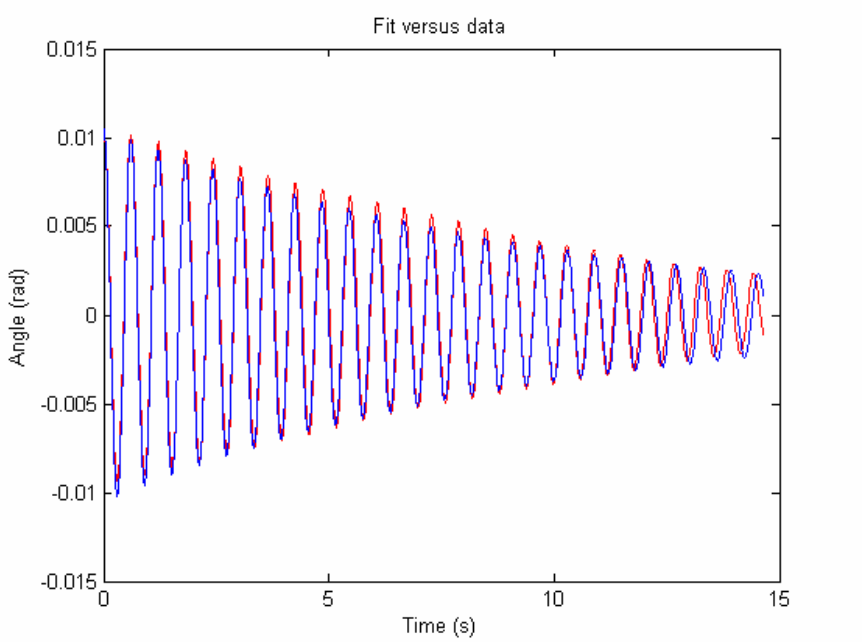

FIGURE 4.3.3 Curve fit showing errors at small angles (red = data, blue = fit)

was just over 1°. Although the OptoTrak system has a high accuracy, the motion of the pendulum in these trials, especially the low and medium force trials, may have been small enough that this error affected them significantly. Since the motion was only recorded for 10 seconds, the high force trials did not record the pendulum's motion at the smaller angles seen in the low and medium force trials. If the angles from the low and medium trials are limited to the range seen in the high force trials, the estimated stiffnesses do not change significantly (<1%). However, in such a case, the fit matches much better (Figure 4.3.4).

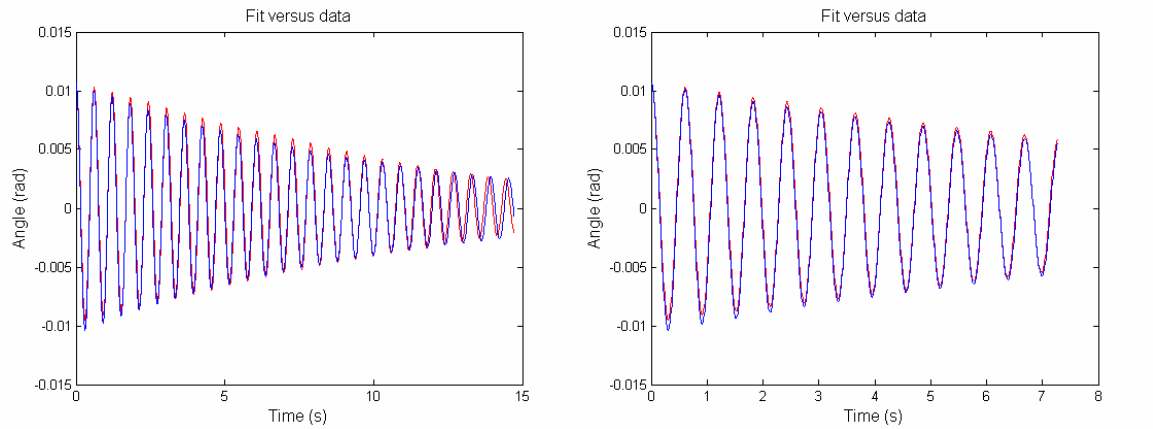

FIGURE 4.3.4 Curve fit for low force trial through end of data (left) and limited (right) (red = data, blue = fit)

In conclusion, our methods for identifying this inverted pendulum estimated the spring's stiffness within 6% of the measured spring stiffness. The damping coefficient was consistent across trials (SD less than 15% of average) and the R^2 values were over 0.9 for every trial. Based upon the success of these trials, we expect to achieve good results when identifying the human head/neck system's stiffness.

CHAPTER FIVE

HUMAN SUBJECTS EXPERIMENTS

5.1 HUMAN SUBJECTS METHODS

The final part of this study was to test the reflex response of the human head/neck system in order to determine the stiffness and damping coefficient of the human neck and the onset latencies for various muscles within the neck. Although the focus of the study was to build and verify the device, testing human subjects is the overall goal of this study and any which may follow it. Therefore, to complete the process preliminary tests were performed on human subjects. This served to establish a protocol for future experiments as well as work through any complications which may arise from working with human subjects.

5.1.1 Subjects

Two subjects volunteered for the study: a 29 year old female (subject 1) and a 23 year old male (subject 2). Although recent studies have been contradictory on whether males and females respond differently to head perturbations [21, 22], we did not focus on a particular gender in this study. Both subjects gave their informed consent. Neither of the subjects had a history of neck trouble. Our study was approved by the Washington State University Institutional Review Board.

5.1.2 Measurements

Anatomical constants needed to complete the analysis of the subject's response include the moment of inertia, the position of the center of gravity, and the mass of the

head and neck. Since these values cannot be measured directly, we used Zatsiorsky and Seluyanov's regression equations (Equations 23-25) to estimate them [27]. Various other approximations exist, but these equations reported high correlation factors and come from the same source. The equations are as follows:

$$I = -983 + 19.9X_1 + 8.43X_2 + 3.22X_3 + 10.2X_4 \quad (23)$$

$$CG = 0.210 + 0.503X_1 + 0.027X_2 + 0.043X_3 - 0.158X_4 \quad (24)$$

$$m = -7.385 + 0.146X_1 + 0.071X_2 + 0.0356X_3 + 0.199X_4 \quad (25)$$

where I is the moment of inertia for the head and neck about the transverse axis in kg-cm^2, CG is the distance from the vertex (top of the head) to the center of gravity for the head and neck in cm, and m is the mass of the head and neck in kg. X_1 is the projected distance between the vertex and the C7 spinous process. It was calculated as the difference between subject's height (floor to vertex) and the distance from the floor to the C7 spinous process. X_2 is the maximal circumference of the head when the head is in the Frankfort plane (approximately looking straight ahead). X_3 is the average of X_2 and the circumference of the neck just below the Adam's apple. X_4 is the maximum diameter of the head from left to right. These constants, as well as the I, m, and CG of the subjects, are shown in table 5.1.1.

TABLE 5.1.1 Anatomical constants for each subject

	Subject 1	Subject 2
Age (yrs)	29	23
Sex	F	M
Body mass (kg)	68.2	85.6
Floor to vertex (cm)	174.8	178.6
Floor to C7 (cm)	149.1	153.5
X1 (cm)	25.7	25.1
X2 (cm)	54.8	58.2
X3 (cm)	44.5	49.4
X4 (cm)	14.3	15.1
I (kg-cm^2)	279.5	320.2
CG (cm)	14.3	14.1
Head/Neck Mass (kg)	4.6	5.1

5.1.3 Electromyographs

Surface electrodes were placed on the subject after the anatomical measurements were completed. They were placed on the right side sternocleidomastoid (SCM), the semispinalis capitis (SEMI), the paraspinal muscles (PARA), and the splenius capitis (SPL). The SCM electrode was placed on the belly of the SCM halfway up the muscle (Figure 5.1.1). The SEMI electrode was placed below the hairline on the back of the neck just lateral to midline. The PARA electrode was placed below the SEMI electrode on the back of the neck, near the level of C5. The SPL electrode was placed in the window on the side of the neck created by the bottom of the SCM and the top of the trapezius muscle. All EMG's were sampled at 1000 Hz. They were amplified by 10,000 during trials and bandpass filtered between 20 and 450 Hz.

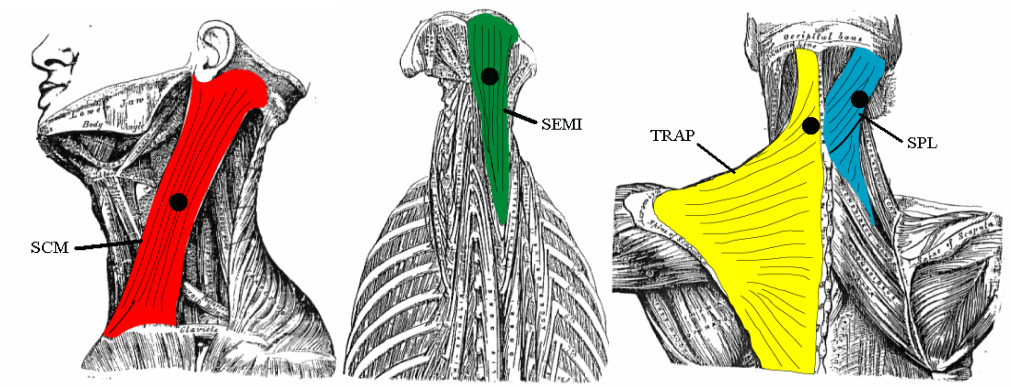

FIGURE 5.1.1 Right to Left: Electrode placement on the SCM, SEMI, SPL, and PARA (shown on the TRAP)

5.1.4 Experimental Protocol

After the EMG's were attached, they were seated in the chair of the experimental apparatus (Figure 5.1.2). A racing harness attached to the chair was used to secure the subject's torso in place. The subject then donned the helmet and swimming goggles. The swimming goggles were painted black to block the subject's vision. Subjects also wore earplugs to stop any audible cues of an impending perturbation. Various studies have shown that knowledge of the timing the perturbation affects the subjects' responses [17, 18]. Blocking the auditory and visual feedback kept the subject unaware of the timing of the perturbation.

FIGURE 5.1.2 Subject in setup

Once the subject was seated and the equipment was adjusted, the subject was instructed to assume their neutral head position. This position was marked and the impacter was moved so that it was between 2 and 3 cm of the block on the helmet. A second investigator was used to confirm that the subject was within this range at the beginning of each trial.

The subject was instructed to relax as much as possible in order to let the natural reflex response occur after the perturbation. The main investigator used a real-time graph of the EMG data to determine if the subject was relaxed. If the subject's EMG did not look relaxed, they were told to relax more. The trial only began when the subject did not show any clear periods of activation in their baseline signals. Once the subject was positioned correctly and relaxed, the trial began after a random delay (described below).

Each trial recording included at least 1 second of baseline data. We refer to all the trials for a given subject in a given direction (e.g. subject 1 flexion) as a block.

5.1.5 Experimental Order

The tests were given in directional groups, 10 in flexion and 10 in extension. The flexion/extension order was reversed between subjects. Since the motor's motion was initiated by clicking the run button in the SMI program, the subjects could potentially hear the noise and tense in anticipation of the test. This was limited by the subject wearing earplugs as stated before. Also, if the impact was initiated at roughly the same delay, the subject might learn to tense, whether subconsciously or consciously, in anticipation of the perturbation. To limit this, five different delays (0, 5, 10, 15, and 20 seconds) were used between when the subject was confirmed as ready and the perturbation began. To make the order random, each delay time was assigned a number, 1 to 5, respectively. The order for the tests was then chosen using these numbers and a random order generator (www.random.org). At the end of the 10 trials, the data were quickly reviewed to confirm that EMG responses were seen in at least 5 trials and the data looked consistent. If this wasn't the case or the investigator or subject felt that a trial needed to be repeated, additional trials were recorded.

5.1.6 Perturbations

The same motor program was used for each subject. The motor was programmed to apply a constant power for a certain amount of time and then return to its initial position. Although the output was constant power, we assumed a constant torque was applied. This is reasonable as long as the motor does not reach a high velocity. For a

small range, the motor's output torque is constant with increasing speed (Figure 3.3.1). During our analysis of the results, we determined the motor's speed did exceed the range mentioned above and thus our assumption was not correct and the torque was not constant.

Extension trials were those in which the head was forced backwards. Flexion was when the head was pushed forward.

5.1.7 Positional Markers

Since it was not possible to find 4 locations on the subject's head on which markers could be attached and remain visible without skin movement, the subject's head motion was defined by the motion of the goggles. A piece of fiberglass was attached to the goggles' left eye-piece. Four positional markers were placed on the piece of fiberglass. These were used to define a rigid body within the OptoTrak system to represent the head's position in space.

In order to verify that the goggle movement was an accurate representation of the head movement, a marker was placed between the subject's eyes during 10 trial runs. The marker's position was recorded while the subject's head was perturbed as in the final tests. We then found the maximum 3-dimensional motion between the marker on the skin and two separate markers on the goggles for each of the runs. These averaged 0.16 mm. Since this was two orders of magnitude less than the average maximum motion of the head (20 mm in the posterior-anterior direction) we decided the goggles were an accurate representation for the head movement.

Four markers were also attached to a rectangular piece of aluminum and used to define a rigid body. The piece was attached to the subject's chest using medical tape.

This was used to measure any motion in the subject's torso during the trials. We subtracted the chest rigid body data from the goggles' rigid body data to determine motion of the head with respect to the chest.

Two final markers were used in the study. One of these was attached to the impacter to record how far it moved during each trial. The other was attached to the helmet. This was used to verify that the helmet stayed relatively stationary with respect to the head during the trials.

All markers were sampled at 100 Hz.

5.1.8 Data Analysis

The load cell output was used to determine the onset of the perturbation for every data file. To determine this onset, the time of maximum force was found for each trial and an algorithm worked backward to find the time when the force value first became less than or equal to 10% of the maximum force. This method was used because most of the force data showed an initial spike around 0.1 seconds before the force was actually applied (Figure 5.1.3). This method avoided the spike.

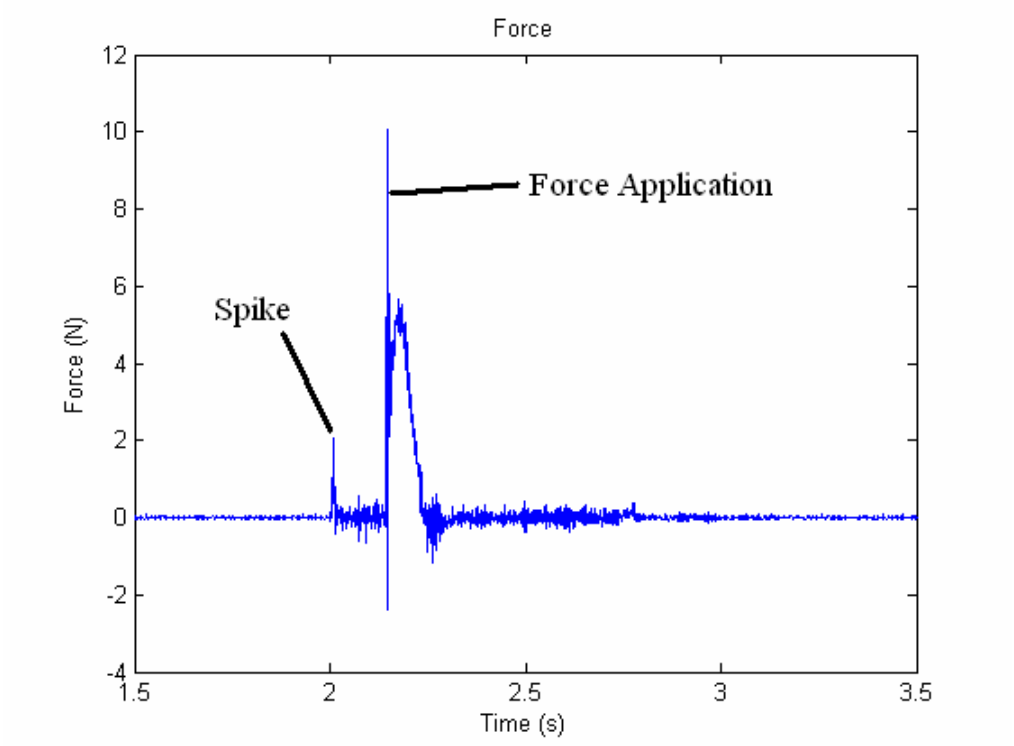

FIGURE 5.1.3 Typical force signal for human subjects experiment

The maximum force in each trial was recorded as well as a 5 point average force. Most of the force data showed an initial peak (usually only one point) followed by a longer bump of lower amplitude lasting about 100 ms. The maximum 5 point moving average, average of 5 consecutive data points, was the amplitude of the longer bump rather than the single point peak.

The maximum motion in the vertical and posterior-anterior directions and the maximum flexion-extension angle of the head with respect to the chest were determined for each trial as well as the time it took the subject to reach peak positions. The data were calculated relative to the average of the 0.5 seconds before the force onset.

The 20 point moving window root mean square (RMS) was found for the detrended EMG data. The average over the 100 ms before the force onset was subtracted

from the data so that the average baseline was defined as no activation. The onset time for the EMG response was then defined as the time after the force onset when the RMS value became greater than or equal to 10% of the maximum RMS value for that trial [15]. Some of the EMG recordings contained blips between the force onset and the clear EMG activation. These blips were considered EMG activation if their maximum value was greater than 7 times the standard deviation of the baseline (the 0.1 seconds of data before the force onset). All findings were confirmed by visual inspection and adjusted as needed.

5.1.9 Statistics

T-tests were performed on both the motion and EMG data to determine whether the results were statistically different in various conditions (directions/subjects). We first checked whether the forces were statistically different between subjects for the same direction (i.e. subject 1 flexion versus subject 2 flexion). For both the maximum force and the 5 point average force, every comparison revealed that the forces were statistically different ($p<0.05$). Based upon these results, we normalized the maximum position data with respect to the force by dividing each position value by the corresponding 5 point average force (this assumes a linear relationship between force and motion which may not exist). Once this was complete, *t*-tests were used to compare the posterior-anterior and angular motion for the same subject between flexion and extension. An α value of 0.05 was chosen for the null hypothesis criteria.

The different muscles' EMG onset latencies were compared within a block to determine if each muscle's onset time was unique from the others. They were also compared between flexion and extension for the same subject.

5.1.10 Test Criteria

The first 3 trials for each subject in each direction were discarded to account for habituation, the subject's adaptation to the perturbations. Siegmund and colleagues found that habituation of the head and neck occurred after only 1 trial [16]. By discarding the first 3 trials, any habituation effects should be eliminated.

In a few of the tests, the motor hit the subject twice. This occurred when the motor did not move back to its original position quick enough and the subject hit the impacter during their stabilization. If this occurred, the trial was not considered.

Other variables were also examined to determine if we should discard a trial. These were the maximum force, the maximum moving average force, the baseline of the EMG signals, the initial linear and angular position for the head, and the initial angular position of the chest. Trials were discarded if any of these variables was more that 2 standard deviations from the average of all the trials in its block.

5.2 HUMAN SUBJECTS RESULTS

Typically, consistent results were obtained in these experiments in that our criteria for discarding trials resulted in only 4 trials being discarded besides the initial 3 for each group of trials. A typical response of a subject is shown in figure 5.2.1.

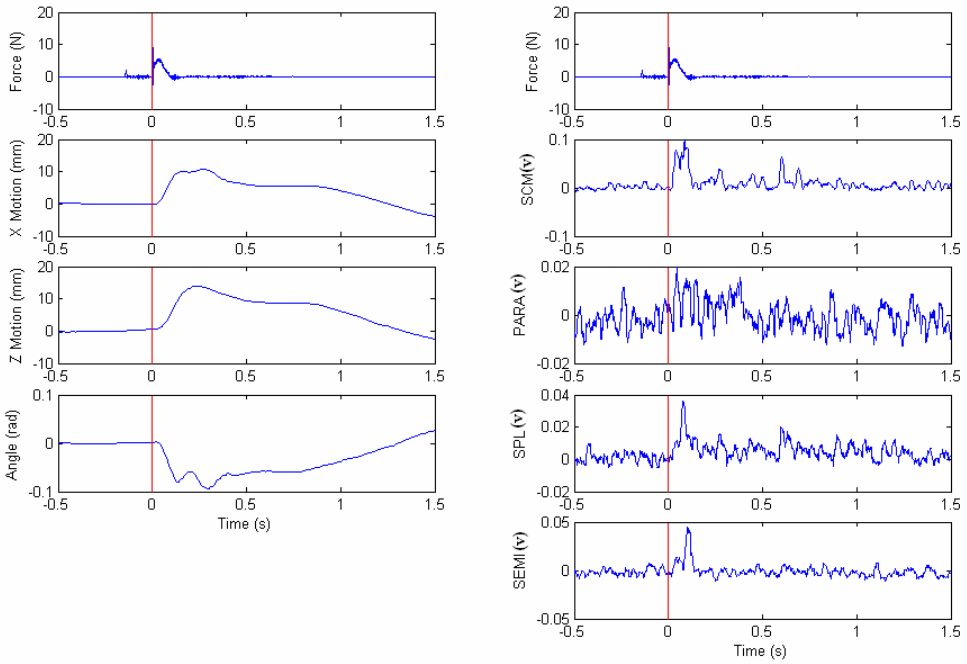

FIGURE 5.2.1 From Top to Bottom: Left Column: Force, head x (vertical, positive is up), head z (anterior-posterior, positive is posterior), and angular (flexion-extension, positive is flexion) motion Right Column: Force, sternocleidomastoid (SCM) EMG, paraspinal (PARA) EMG, splenius capitis (SPL) EMG, and semispinalis capitis (SEMI) EMG versus time for a typical extension trial (Force onset is at time 0)

5.2.1 Force and Motion

As stated before, the forces applied varied depending on the subject and the direction of the tests (Table 5.2.1). There did not appear to be a correlation between force and motion. The maximum and 5 point average force were both statistically different between subjects within directions. Because of this, we did not group subjects together.

TABLE 5.2.1 Summary motion and force data (mean ± s.d.) for both subjects

	Subject 1		Subject 2	
Direction	Flexion	Extension	Flexion	Extension
Max Average Force (N)	4.80 ± 0.15	5.46 ± 0.25	7.35 ± 0.14	10.59 ± 0.41
Max Force (N)	12.39 ± 0.88	8.42 ± 1.78	9.50 ± 1.34	12.67 ± 1.25
Max Absolute X Motion (mm)	21.02 ± 5.88	10.15 ± 1.49	11.51 ± 1.93	17.54 ± 4.03
Time To Max X (s)	0.335 ± 0.051	0.258 ± 0.064	0.226 ± 0.048	0.325 ± 0.087
Max Absolute Z Motion (mm)	19.37 ± 4.40	13.61 ± 1.75	10.81 ± 1.14	19.36 ± 4.85
Time To Max Z (s)	0.328 ± 0.055	0.238 ± 0.016	0.199 ± 0.022	0.325 ± 0.083
Max Absolute Angle (°)	8.96 ± 2.60	5.08 ± 0.58	4.48 ± 0.84	7.61 ± 1.97
Time To Max Angle (s)	0.337 ± 0.052	0.264 ± 0.077	0.214 ± 0.067	0.318 ± 0.112

The maximum average motion in the anterior-posterior direction ranged between around 10.5 and 19.5 mm with subject 1's flexion the highest and subject 2's flexion the lowest. The maximum average angle ranged from about 4.5° and 9.0°. The averages of the maximum average force ranged between about 5 and 10.5 N.

Normalizing the data did not change the patterns within it much. Subject 1's force-normalized angle and posterior-anterior motion (Table 5.2.2) were significantly larger in flexion than extension ($p<0.05$). Subject 2's force-normalized anterior-posterior motion, however, was significantly larger in extension than flexion. Subject 2's average angular motion was larger in extension as well but not significantly different from the flexion average. The data from the 2 subjects were not grouped since *t*-tests revealed they were statistically different.

TABLE 5.2.2 Force normalized posterior-anterior motion and flexion-extension angle

	Subject 1		Subject 2	
Direction	Flexion	Extension	Flexion	Extension
Max Absolute Motion (mm/N)	4.03 ± 0.98	2.62 ± 0.38	1.45 ± 0.17	1.81 ± 0.46
Max Absolute Angle (°/N)	1.87 ± 0.56	0.94 ± 0.15	0.61 ± 0.11	0.72 ± 0.18

The basic response of the subject was similar across trials within a group (Figure 5.2.2) although the magnitudes were different.

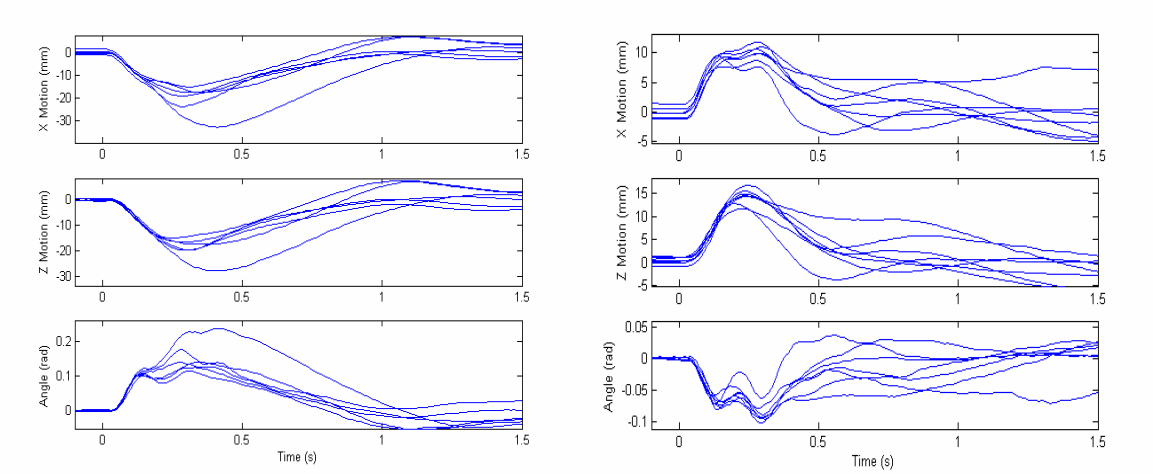

FIGURE 5.2.2 From Top to Bottom: x (vertical, positive is up), z (posterior-anterior, positive is anterior), and angular motion for all trials of subject 1 flexion (left) and extension (right) (Force onset at time 0)

There was no apparent relationship between trial number and motion or force (Figure 5.2.3).

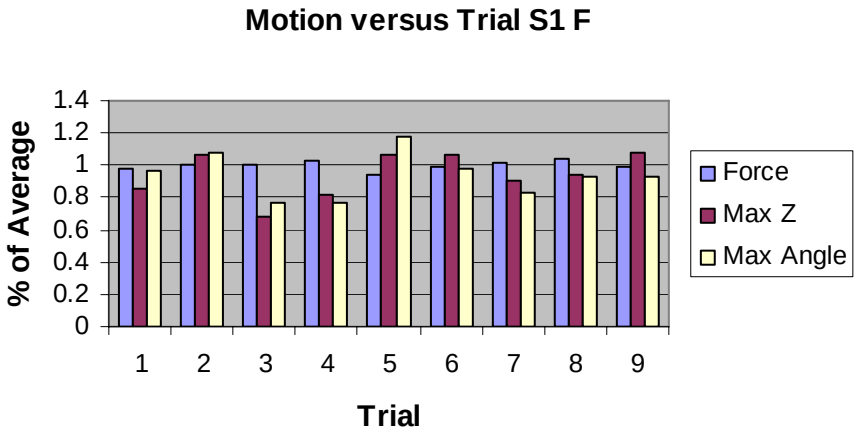

FIGURE 5.2.3 Bar plot of maximum motion (z is posterior-anterior) and force (5 point average) versus trial number for subject 1 flexion

5.2.2 Muscle Onset Latencies

The onset latencies (Figure 5.2.4) for these trials averaged between 20 and 90 ms. Subject 1 had too few responses for SCM in flexion and those data were ignored. Both subjects had the same order of average onset latency in flexion in the extensor muscles. This was SEMI, then PARA, and then SPL from fastest to slowest. They both also had SCM and SPL as the fastest and second fastest onsets in extension, respectively. Subject 1 showed SEMI as the next fastest while subject 2 showed PARA (Table 5.2.3).

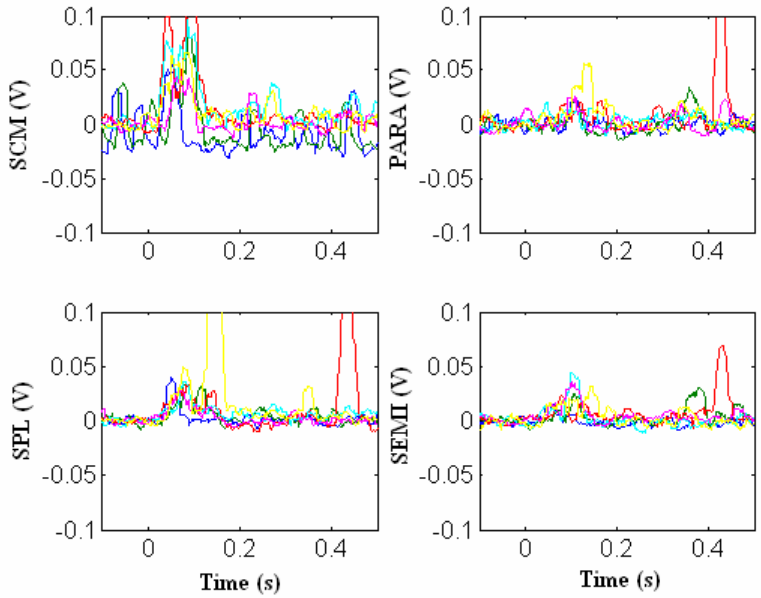

FIGURE 5.2.4 EMG overlays for a subject 1 extension trial (Force onset at time 0)

TABLE 5.2.3 Onset latencies for the neck muscles

	Subject 1		Subject 2	
	Flexion	Extension	Flexion	Extension
SCM	Does Not Apply	22 ± 9	85 ± 15	32 ± 4
PARA	37 ± 9	66 ± 24	41 ± 11	68 ± 11
SPL	41 ± 12	27 ± 12	51 ± 5	56 ±24
SEMI	32 ± 8	43 ± 25	36 ± 11	75 ± 6

The EMG data also were not grouped between subjects because *t*-tests revealed that most of the muscles were different between subjects in extension. None of the muscles were different between subjects in flexion. However, for each subject, onset latencies were also compared between flexion and extension. Subject 1 showed only the PARA muscles as different between flexion and extension. Subject 2 showed all but the SPL were different between the directions.

The between muscle *t*-tests revealed that onset latencies were not statistically different for any muscles for subject 1 in flexion. The PARA was different from the SCM and SPL muscles for the extension trials. Subject 2 showed more differences between flexion and extension. In flexion, the SCM was different from all the other muscles and the SPL and SEMI were also different from each other. In extension, the SCM was different from the PARA and SEMI muscles.

5.3 HUMAN SUBJECTS DISCUSSION

The original goal of this study was to determine the stiffness and damping coefficient of the head/neck system through system identification. To do this, we assumed the head/neck system was a linear, second order system. Upon analyzing the human subject trials' data, we concluded that, for our trials, the head/neck could not be accurately represented by a linear second order system.

The system displays properties of a second order system briefly (Figure 5.3.1). The motion moves to a forced peak at the beginning. The subject then recovers and there is, in a few trials, one or two oscillations as we would expect in a non-overdamped second order system. One problem is that these oscillations are not about the subject's

initial position. Another problem is the dip in the angular data during its upslope as seen below. This dip corresponds to the force offset so that it seems the subject first moves in the opposite direction and then continues as normal when the force stops being applied.

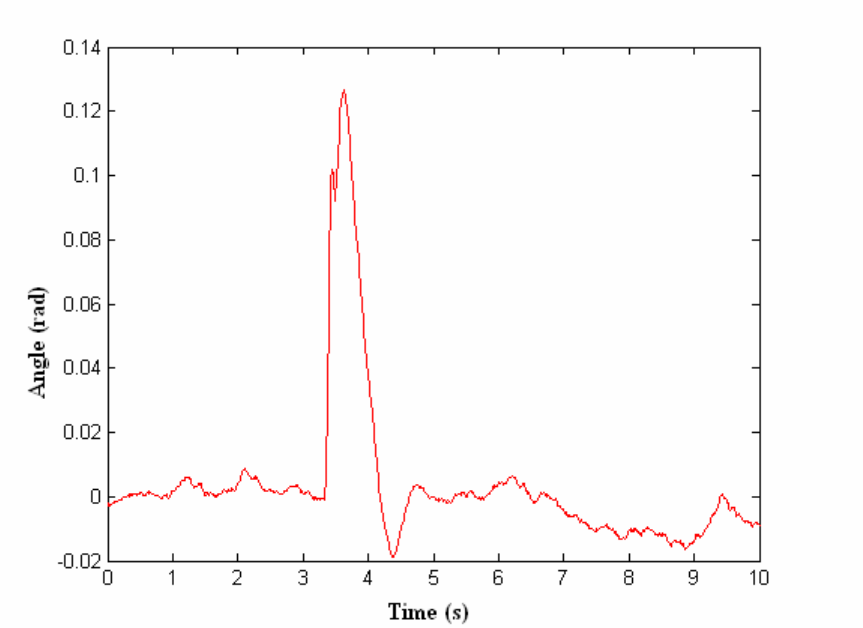

FIGURE 5.3.1 Angular (head with respect to chest) data showing second order-like oscillations

The main reason our results should not be approximated as a linear second order system is that the motion lasts long enough that voluntary reactions may be occurring. Other researchers have found voluntary reactions at around 100 ms after the perturbation [24]. In our trials, the subjects reached their peak position on average after 280 ms; thus, voluntary control likely affected their positional data. We also see EMG modulation before the motion is completed. Thus, the conditions were changing during the subjects' responses and the linear condition is no longer met.

Initially, we decided to try using the method of logarithmic decrement (described in section 4.1) to obtain the damping coefficient and stiffness of the system based upon

the peaks of the oscillations we found. However, some trials showed no oscillations and those that did have oscillations had too few to perform an accurate analysis. The fact that they were not about the initial position also deterred us. Therefore, we did not use the logarithmic decrement method either.

One possibility which future work should examine is that our motion was simply too large for the second order estimation of the head/neck to apply. Tangorra and colleagues [2] rarely, if ever, displaced the head more than 5°. Most of our trials showed more motion than this (overall average of 6.7°). This may have made the linear model assumption inaccurate.

5.3.1 Helmet Motion

Although the helmet was designed to remain motionless with respect to the head, motion did occur between the helmet and the goggle rigid body. The maximum average helmet motion was 1.74 mm which is nearly 10% of the overall head motion, 19 mm. This may have affected our results in that all of the applied force was not transferred to the head. Subject 1's helmet moved much more than subject 2 on average. This may be caused by tightening the helmet more for subject 2 than subject 1 or it may be that subject 2's head geometry fit the helmet better which allowed the helmet to grip the head better. It also may be because of differences in the skin motion between subjects. Since the skin on a person's forehead can move with respect to the skull and the helmet uses this skin as the contact point, the helmet can move with respect to the skull. There is no apparent fix for these possible problems besides making sure the helmet is tightened as much as possible without causing the subject discomfort.

5.3.2 Force

The range of forces, 5 to 11 N, was similar to that in other studies. Most of the other studies which applied a force [19, 21, 22] used a 1 kg weight that was either dropped or moved to apply the perturbation. This would yield a force of 9.81 N which falls within the range of forces we saw.

Although the motor parameters were the same, the range of recorded forces was broad. This could be caused by the motor sending a different signal, the helmet moving more in some trials than others, or the subject's response to the force. There was no relationship between how far the impacter moved and the force recorded in the trial. There was also no relationship between how far the helmet moved with respect to the head and the force. These would seem to be the easiest explanations for the range of forces we saw however, since there is no relationship, they do not account for it. The range may just be caused by the different responses to the perturbations. Since there must always be an equal and opposite force, if the subject was less stiff or had a larger damping coefficient in one trial than another, the maximum force value would drop. The force was larger for both subjects in the first block they underwent. This may be happenstance or it may show habituation in the subjects.

As stated before, there did not appear to be any relationship between force and motion. Since the muscle activation pattern and thus the stiffness of the system changed between trials, applying the same force to the same subject may cause completely different reactions based on the muscle activation. This would explain the lack of a relationship.

5.3.3 Motion

Since we could not determine the system's stiffness or damping coefficient, we analyzed only the various motion parameters discussed above. As mentioned before, subject 1 had more motion in flexion while subject 2 had more motion in extension. Differing muscle responses and differences in neck kinematics and stiffness may have caused this difference between subjects. Neck kinematics differences may have been caused by one of the subjects moving more in translation than rotation during one block. This can be seen in the angular data from the trials (Figure 5.2.3). In both flexion and extension, there is a dip in the angular motion while the posterior-anterior motion continues to increase. This may show a moment of translational motion rather than angular. We would expect the subjects to be stiffer in flexion trials than extension due to the larger extensor muscle mass

It was also interesting to note that there was no apparent relationship between force and maximum motion. This shows the variability associated with physiological systems as opposed to mechanical systems. Again, the muscle responses may have caused this. Different muscle responses between would change the motion of the head so that the force would not directly affect the maximum motion.

Since there also seemed to be no relationship between maximum motion and trial number, there may be a lack of habituation in our trials. More analysis is required to completely rule this out.

5.3.4 Onset Latencies

The reflexive onset latencies reported in the other studies covered in this paper were between 20 and 80 ms [12-22]. Mazzini and Schieppati [24] showed voluntary

responses at just over 100 ms. Because of these findings, we decided that any result over 100 ms represents voluntary reactions. The only exception to this was subject 2's SCM during flexion. One of the onset latencies from this group was 105 ms. Since many of the other latencies for this muscle in flexion were in the 90-100 ms range, we decided not to ignore this result. This muscle, subject 2 flexion SCM, was the only muscle that showed average onset latency outside of the range others reported. These results could all be voluntary as well. Subject 2's SEMI in extension was close but still fell within the range. Since we obtained results similar to other past studies, we feel more confident with our results.

Some of our trials showed 2 peaks in the EMG responses. Corna [14] also noted this. They attributed this to 2 different pathways, vestibular (20 to 30 ms) and stretch (55 to 70). We did not determine the onset of the later peak and so did not differentiate between the normal pathways in this study.

Although the average onsets followed a pattern between muscles in both directions for both subjects, statistically most of these were not different and so we cannot conclude about the order of response for most of the muscles. For subject 2 in flexion, we can say that the SCM response lagged behind all the other muscles. This is to be expected as the SCM is a flexor and would not respond except to provide co-contraction (activation of opposite direction muscles to stiffen a joint) in the flexion trials.

Subject 2 showed a difference in 3 of the 4 muscles between flexion and extension while subject 1 only showed a difference in 1, so we cannot make any conclusions about whether a difference exists in the onset latencies of these muscles

between flexion and extension trials but, given subject 2's results, we would expect a difference.

Since the time to maximum motion was in the hundreds of ms and the onset latencies were all below 100 ms, all of the muscles reacted during the initial forward or initial backward motion of the head. For forward motion of the head, flexion trials, this means that in every trial that the SCM activates, it is co-contracting. Likewise, in extension trials, whenever the SEMI, SPL, or PARA muscles activate, they are co-contracting as well. It also shows that by the time the subjects stop and start to return to normal position, they have most likely begun voluntary control.

Subject 1 had only two usable onset latencies for the SCM in flexion. The other tests either had the SCM unresponsive or showed only activation with a delay long enough to be voluntary. As such, the t-tests involving these data are less significant and we cannot make any conclusions about the SCM's response in this circumstance. This is not surprising since we would not expect the SCM to respond during flexion trials.

One problem commonly associated with surface EMG for the SPL is that of cross-talk between it and other muscles. Since the window where the SPL is the most superficial muscle lies between the trapezius muscle and the SCM, often their signals will interfere with the SPL's. Since the SPL and SCM's onset latencies were statistically different in only 1 of the 4 trial groups, we cannot determine if crosstalk was occurring in the other trials. More analysis is required to determine if this is occurring.

In conclusion, our results showed that the human head/neck system is not a second order system. The results also showed variation between whether the subject moved more in flexion or extension. Our muscle onsets were within the range of other

studies and again showed discrepancy between subjects although the results did seem to suggest the muscles reacted differently between flexion and extension.

CHAPTER SIX

RESULTS/FUTURE WORK

The goals for this study were as follows:

1. Develop an experimental setup which will allow for perturbations to be safely applied to a seated subject's head in any direction in the horizontal plane.
2. Test this system to verify that it can calculate the stiffness and damping properties of an inverted pendulum.
3. Use this system to study the reflex response and characterize the stiffness of the human head/neck system in flexion and extension.
4. Use this system to determine the onset latencies for major neck muscles.

These goals were accomplished.

The experimental setup we developed consists of a free-standing frame which allows the head to be perturbed from any direction in the horizontal plane. The setup uses a load cell to measure the force applied, a 3D positioning system to record the motion, and EMG's to record the muscle activity. Two safety stops were built into the setup, limit switches for the motor and a master kill switch. These ensured the safety of the subject during the trials.

The frame proved stiff enough for our applications once cables were attached. During trial runs, the frame moved less than 1% of what the force applicator moved. This met our criteria.

We used the setup to identify the stiffness of an inverted pendulum using system identification. The average calculated stiffness of the spring in the setup, 1427.1 N/m,

was only 6% higher than the measured stiffness, 1346.1 N/m. The damping coefficient was consistent.

We successfully used our setup to apply a force to a human subject and record the reflexive response. Although the human head/neck system shows limited second order characteristics, it was not a second order system. Because of this the stiffness of the head/neck system was not determined. However, the neck muscle onset latencies and comparative head motions were measured.

Neck muscle onset latencies were in the range of previous studies, 22 to 85 ms compared to 20 to 80 ms [12-22]. We also found evidence that the latencies vary between flexion and extension.

We tested two subjects, who responded differently during the tests. Subject 1 had more motion in flexion while subject 2 had more in extension. This probably represented different response strategies within the central nervous system.

By including more subjects in future studies, investigators could make conclusions about things like how women respond differently to head perturbations than men or whether there is a difference in the positional and muscular responses between flexion and extension. With more subjects, the investigators may also find data that are closer to a second order system. If this occurs, investigators could estimate the stiffness and damping coefficient of the human head/neck. Both of these changes would lead to a better understanding of the head/neck system.

It would also be helpful to investigate the responses with lower forces. Since our maximum angular displacement was more than 5°, an estimate for where the head/neck

system loses its linearity [2], future investigators may see a second order system if they reduce the motion of the subjects.

Overall, our study was a success. We successfully built and tested a device that can apply perturbations to a subjects head and accurately record their responses. We successfully tested a known second order system and determined a relatively accurate stiffness and consistent damping coefficient. We then successfully tested two human subjects even though we showed that one of our assumptions was not correct. Future work in this study should provide more insight into the reflex responses of the human head/neck system.

APPENDIX A

References:

1. Fard, Mohammad A., Ishihara, Tadashi and Inooka, Hikaru (2003) "Dynamics of the Head-Neck Complex in Response to the Trunk Horizontal Vibration: Modeling and Identification." Journal of Biomechanical Engineering. 125(4): p. 533-539.

2. Tangorra, James L., Jones, Lynnette A., Hunter, Ian W. (2003). "Dynamics of the Human Head-Neck System in the Horizontal Plane: Joint Properties with Respect to a Static Torque." Annals of Biomedical Engineering. 31: 606-620.

3. Peng, G.C.Y., Hain, T.C., Peterson, B.W. (1996). "A Dynamical Model for Reflex Activated Head Movements in the Horizontal Plane." Biological Cybernetics. 75: 309-319.

4. http://training.seer.cancer.gov/module_anatomy/unit1_3_terminology2_planes.html

5. http://cara.gsu.edu/calendar/may2002.htm

6. Gray, Henry, Anatomy of the Human Body. Lea & Febiger, Philadelphia PA (1918).

7. Vasavada, A., Siping, L., Delp, S. (1998) "Influence of Muscle Morphometry and Moment Arms on the Moment-Generating Capacity of Human Neck Muscles." Spine. 23(4): p. 412-422.

8. http://www.mucslemag.com/images/illu_muscle_structure.jpg

9. http://faculty.etsu.edu/currie/images/muscle3.jpg

10. McMahon, Thomas A. Muscles, Reflexes, and Locomotion. Princeton University Press, Princeton NJ, pp. 67 (1984).

11. Kendall, Eric R., Schwartz, James H., Jessell, Thomas M. Principles of Neural Science. Appleton & Lange, Stamford CT (1993).

12. Ito, Y. Corna, S., Brevern, M von, Bronstein, A., Rothwell, J., Gresty, M. (1995) "Neck Muscle Responses to Abrupt Free Fall of the Head: Comparison of Normal with Labyrinthine-Defective Human Subjects." Journal of Physiology. 489(3): p. 911-916.

13. Ito, Y. Corna, S., Brevern, M von, Bronstein, A., Gresty, M. (1997) "The Functional Effectiveness of Neck Muscle Reflexes for Head-Righting in Response to Sudden Fall." Experimental Brain Research. 117(2): p. 266-272.

14. Corna, S., Ito, Y., Brevern, M von, Bronstein, A., Gresty, M. (1996) "Reflex Unloading and Defensive Capitulation Responses in Human Neck Muscle." Journal of Physiology. 496(2): p. 589-596.

15. Siegmund, Gunter P., Sanderson, David J., J. Timothy. (2002) "The Effect of Perturbation Acceleration and Advance Warning on the Neck Postural Responses of Seated Subjects." Experimental Brain Research. 144(3): p. 314-321.

16. Siegmund, Gunter P., Sanderson, David J., Myers, Darry S., Inglis, J. Timothy (2003) "Rapid Neck Muscle Adaptation Alters the Head Kinematics of Aware and Unaware Subjects Undergoing Multiple Whiplash-Like Perturbations." Journal of Biomechanics. 36(4): p. 473-482.

17. Blouin, Jean-Sebastian, Descarreaux, Matin, Belanger-Gravel, Ariane, Simoneau, Martin, Teasdale, Norman (2003) "Self-Initiating a Seated Perturbation Modifies the Neck Postural Responses in Humans." Neuroscience Letters. 347(1): p. 1-4.

18. Kuramochi, R., Kimura, T., Nakazawa, K., Akai, M., Torii, S., S Suzuki (2004) "Anticipatory modulation of neck muscle reflex responses induced by mechanical perturbations of the human forehead." Neuroscience Letters. 366(2): p. 206-210.

19. Horak, F., Shupert, C., Dietz, V., Horstmann, G. (1994) "Vestibular and Somatosensory Contributions to Responses to Head and Body Displacements in Stance." Experimental Brain Research. 100(1): p. 93-106.

20. Schupert, C., Horak, F. (1996) "Effects of Vestibular Loss on Head Stabilization in Response to Head and Body Perturbations." Journal of Vestibular Research. 6(6): p. 423-437.

21. Tierney R, Sitler, M., Swanik B, Swanik K, Higgins M (2005) "Gender Differences in Head-Neck Segment Dynamic Stabilization During Head Acceleration." Medicine & Science in Sports & Exercise. 37(2): p. 272-279.

22. Mansell J, Tierney, R., Sitler M, Swanik K, Stearne M (2005) "Resistance Training and Head-Neck Segment Dynamic Stabilization in Male and Female Collegiate Soccer Players." Journal of Athletic Training. 40(4): p. 310-319.

23. Guitton, D., Kearney, R.E., Wereley, N., Peterson, B.W., (1986) "Visual, Vestibular, and Voluntary Contributions to Human Head Stabilization." Experimental Brain Research. 64(1): p. 59-69.

24. Mazzini, L., Schieppati, M. (1992) "Activation of the Neck Muscles from the Ipsi- or Contralateral Hemisphere During Voluntary Head Movements in Humans. A Reaction-Time Study." Electroencephalography and Clinical Neurophysiology. 85(3): p. 183-189.

25. Keshner, E. A., Peterson, B.W. (1995) “Mechanisms Controlling Human Head Stabilization. I. Head-Neck Dynamics During Random Rotations in the Horizontal Plane.” Journal of Neurophysiology. 73(6): p. 2293-2301.

26. Keshner, E. A., Cromwell, R.L., B. W. Peterson (1995) “Mechanisms Controlling Human Head Stabilization. II. Head-Neck Characteristics During Random Rotations in the Vertical Plane.” Journal of Neurophysiology. 73(6): p. 2302-2312.

27. Zatsiorsky, V., Seluyano, V. (1983) “Estimation of the Mass and Inertial Characteristics of the Human Body by Means of the Best Predictive Regression Equations.” Biomechanics VII-B Human Kinetics Publisher.

APPENDIX B

Procedure:

1. Turn on OptoTrak, motor, and EMG systems
2. Open Toolbench and SMI programs
3. Before subject arrives, realign wall rigid body with new camera file
4. Test fire
5. Have subjects sign consent form and explain experiment including safety features and expected motion
6. Take subjects measurements
    a. Age
    b. Gender
    c. Weight
    d. Height
    e. Floor to C7
    f. Floor to sternal notch
    g. Floor to tragus
    h. Maximal horizontal circumference of the head, measured with the head in the Frankfort plane
    i. Circumference of the neck measured beneath the thyroid cartilage
    j. Head diameter measured in the mediolateral direction
7. Have subject climb onto shelf and explain max force trials to subject
8. Connect EMG's to subject
9. Test EMG's by having the subject rotate their head in various directions while you record the EMG's
10. Plot the EMG signals using MatLab to confirm that there is a good signal
11. Record maximum force trials for all the muscles being studied in flexion and extension
12. If necessary repeat steps 8-10
13. Put goggles and chest rigid body on subject
14. Sit subject in chair and strap them in. Adjust chair's position so subject is centered under the frame and adjust slider/impacter so subject's neutral position is 2-3 cm from impacter. Mark neutral position.
15. Take a 5 second trial of markers and make rigid bodies for experiment
    a. Use Toolbench program
    b. Use RigMaker to make rigid body files
    c. Copy and paste the files into the Experiments\Final folder

*** Subject is now free to remove goggles**

16. Have the subject put the goggles, earplugs, and helmet on
17. Use Toolbench to check once more that everything is working fine
18. Hand subject the kill switch
19. Do one trial run of motor program to confirm that it works right and show subject what to expect during the tests. Record this trial.
20. Perform 10 extension trials
    a. Wait 30 seconds to 1 minute between trials
    b. Vary delay period
        i. 0, 5, 10, 15, and 20 seconds
        ii. Randomize order using random sequence generator

        iii. Throw in blank fires as well
        iv. Continue until 10 actual trials were performed
    c. Before next trial, confirm that subject is in neutral position through laser dot and have helper confirm subject is correct distance from load cell
21. Have subject remove goggles, loosen helmet, and sit comfortably
22. Determine basic parameters for each trial checking to confirm that every trial looks normal
23. If necessary repeat steps 18-20
24. Remove marker from impacter and rotate the device
25. Repeat steps 15-18 with flexion
26. Disconnect everything from the subject

Measurement Recording Sheet for Human Subjects Experiments

Subject #: ___2_____ Date: __9/11/6_____

Subject Age: _____ Gender: _____

Weight: _____ (kg)

Heights (cm)
Floor to Vertex: _____

Floor to C7: _____

Floor to Sternal Notch: _____

Floor to Tragus: R_____ L_____

Other Measurements (cm)
Maximum horizontal circumference of head in Frankfurt plane: _____

Circumference of the neck below the thyroid cartilage: _____

Head diameter in mediolateral direction: _____

Strength Trials: Max Force (N) and Length of Test (s)
Flexion
Trial #_____ Trial #_____ Trial #_____

Extension:
Trial #_____ Trial #_____ Trial #_____

Gains and Muscles
Muscle 1: _____ Max Gain: _____ Test Gain: _____
Muscle 2: _____ Max Gain: _____ Test Gain: _____
Muscle 3: _____ Max Gain: _____ Test Gain: _____
Muscle 4: _____ Max Gain: _____ Test Gain: _____

Order Used:
1 = 0 seconds 2 = 5 seconds 3 = 10 seconds 4 = 15 seconds 5 = 20 seconds

From website got order:
Flexion: Trials _____
Extension: Trials _____

APPENDIX C

ENTIRE SETUP

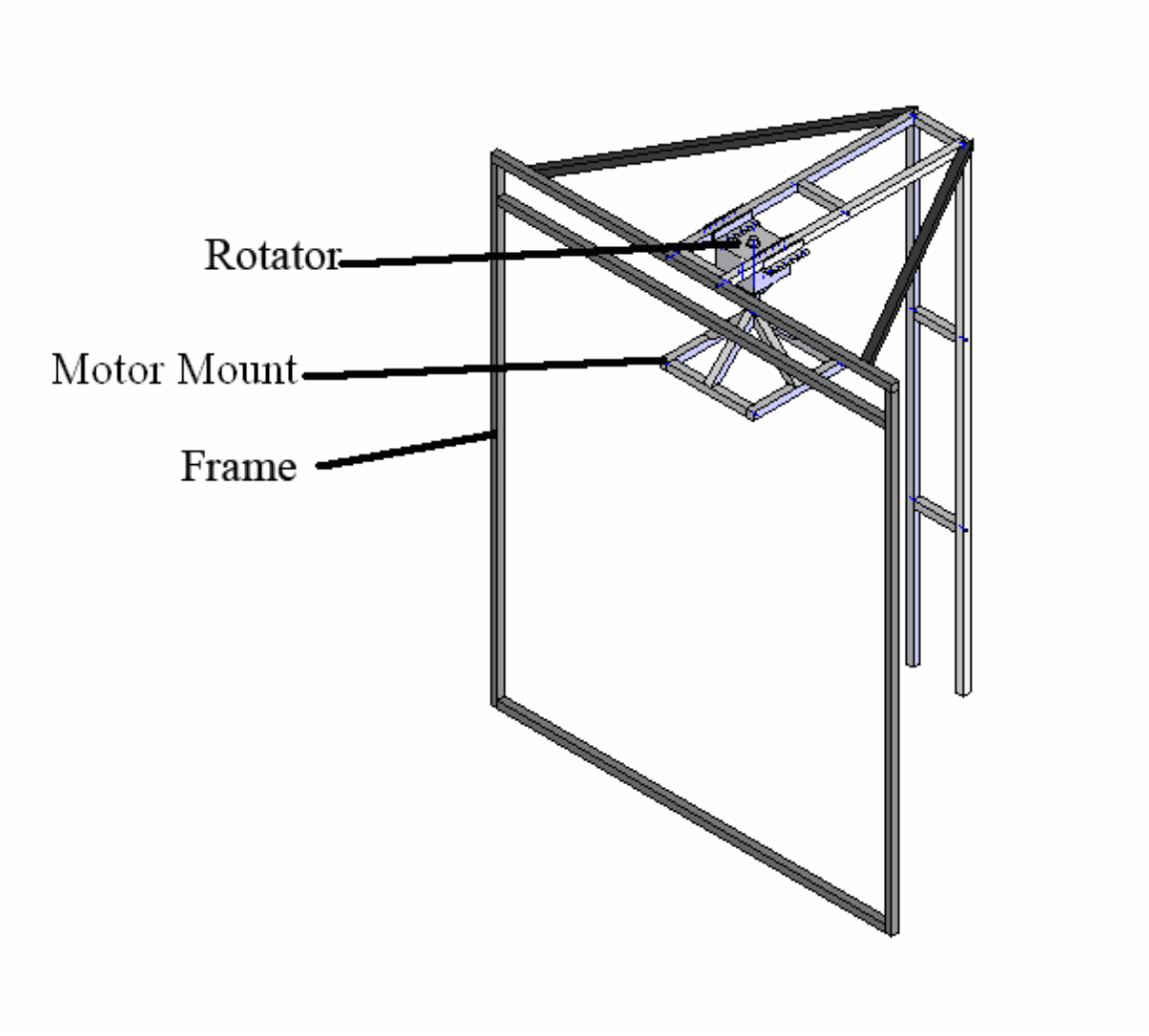

FRAME ONLY

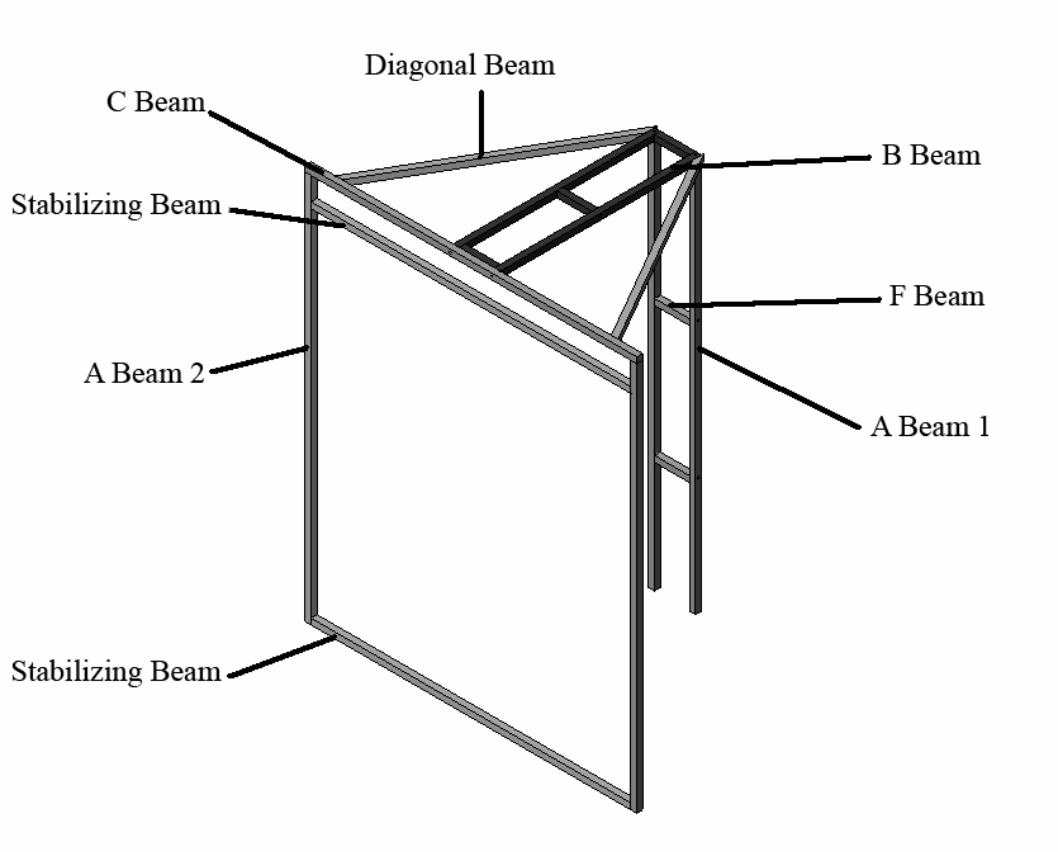
Diagonal Beam
C Beam
B Beam
Stabilizing Beam
F Beam
A Beam 2
A Beam 1
Stabilizing Beam

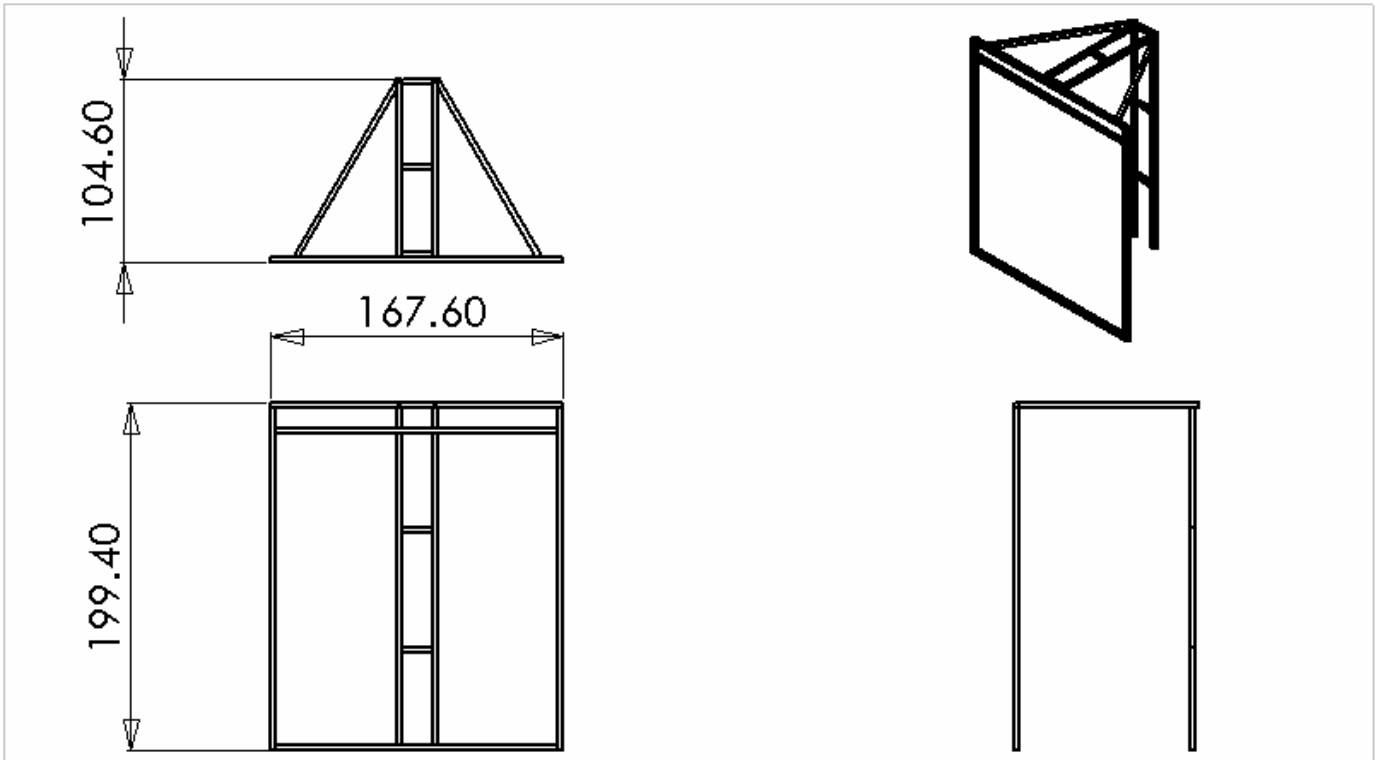

UNLESS OTHERWISE SPECIFIED:		NAME	DATE	Gerald Lucas	
DIMENSIONS ARE IN MM TOLERANCES: FRACTIONAL ± ANGULAR: MACH ± BEND ± TWO PLACE DECIMAL ±0.05 THREE PLACE DECIMAL ±	DRAWN			TITLE:	
	CHECKED				
	ENG APPR.				
	MFG APPR.				
	Q.A.				
INTERPRET GEOMETRIC TOLERANCING PER:	COMMENTS:			SIZE: A	DWG. NO.: Frame
MATERIAL					REV: 9/25/6
FINISH				SCALE: 1:50	WEIGHT:
DO NOT SCALE DRAWING					SHEET 1 OF 1

NEXT ASSY | USED ON | APPLICATION

5 4 3 2 1

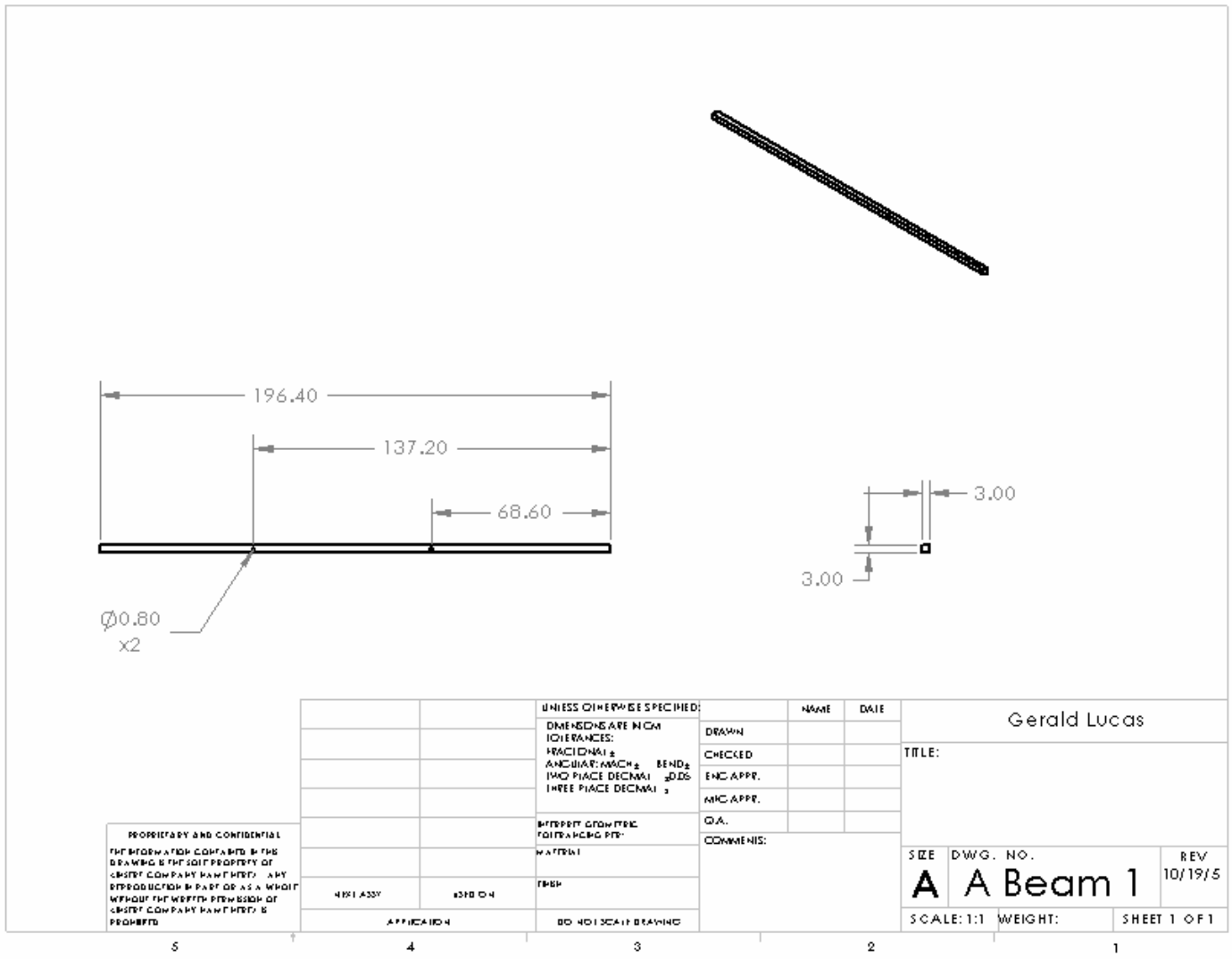
196.40
137.20
68.60
Ø0.80
x2
3.00
3.00
UNLESS OTHERWISE SPECIFIED:
DIMENSIONS ARE IN MM
TOLERANCES:
FRACTIONAL ±
ANGULAR: MACH ± BEND ±
TWO PLACE DECIMAL ±0.05
THREE PLACE DECIMAL ±
INTERPRET GEOMETRIC TOLERANCING PER:
MATERIAL
FINISH
NEXT ASSY
USED ON
APPLICATION
DO NOT SCALE DRAWING
NAME
DATE
DRAWN
CHECKED
ENG APPR.
MFG APPR.
Q.A.
COMMENTS:
Gerald Lucas
TITLE:
SIZE
A
DWG. NO.
A Beam 1
REV
10/19/5
SCALE: 1:1
WEIGHT:
SHEET 1 OF 1
PROPRIETARY AND CONFIDENTIAL
THE INFORMATION CONTAINED IN THIS DRAWING IS THE SOLE PROPERTY OF <INSERT COMPANY NAME HERE>. ANY REPRODUCTION IN PART OR AS A WHOLE WITHOUT THE WRITTEN PERMISSION OF <INSERT COMPANY NAME HERE> IS PROHIBITED.
5
4
3
2
1

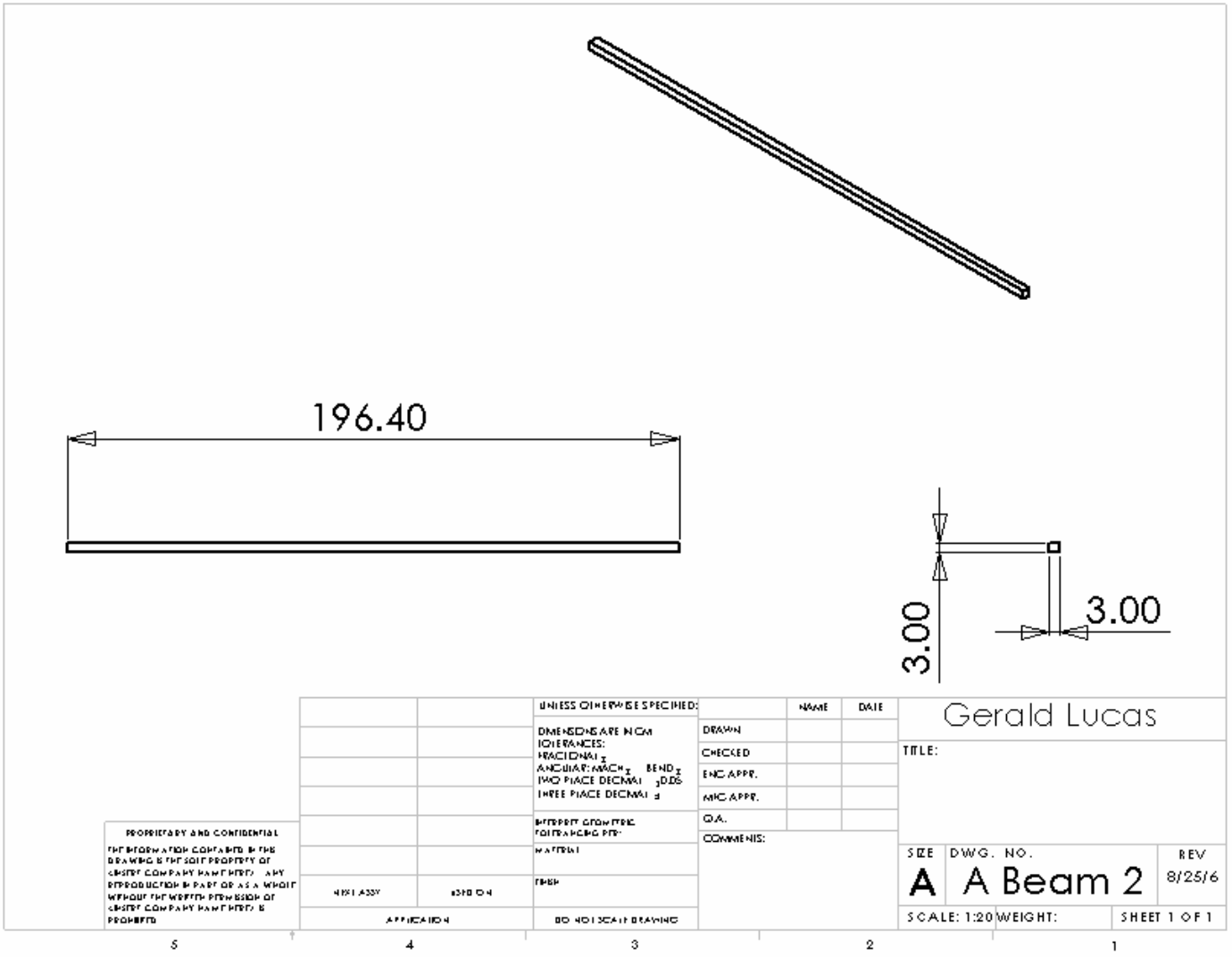

UNLESS OTHERWISE SPECIFIED:		NAME	DATE	Gerald Lucas	
DIMENSIONS ARE IN MM TOLERANCES: FRACTIONAL ± ANGULAR: MACH ± BEND ± TWO PLACE DECIMAL ±0.05 THREE PLACE DECIMAL ±	DRAWN			TITLE:	
	CHECKED				
	ENG APPR.				
	MFG APPR.				
	Q.A.				
INTERPRET GEOMETRIC TOLERANCING PER:	COMMENTS:			SIZE: A	DWG. NO.: A Beam 2
MATERIAL					REV: 8/25/6
FINISH				SCALE: 1:20	WEIGHT:
NEXT ASSY	USED ON				SHEET 1 OF 1
APPLICATION	DO NOT SCALE DRAWING				

5 4 3 2 1

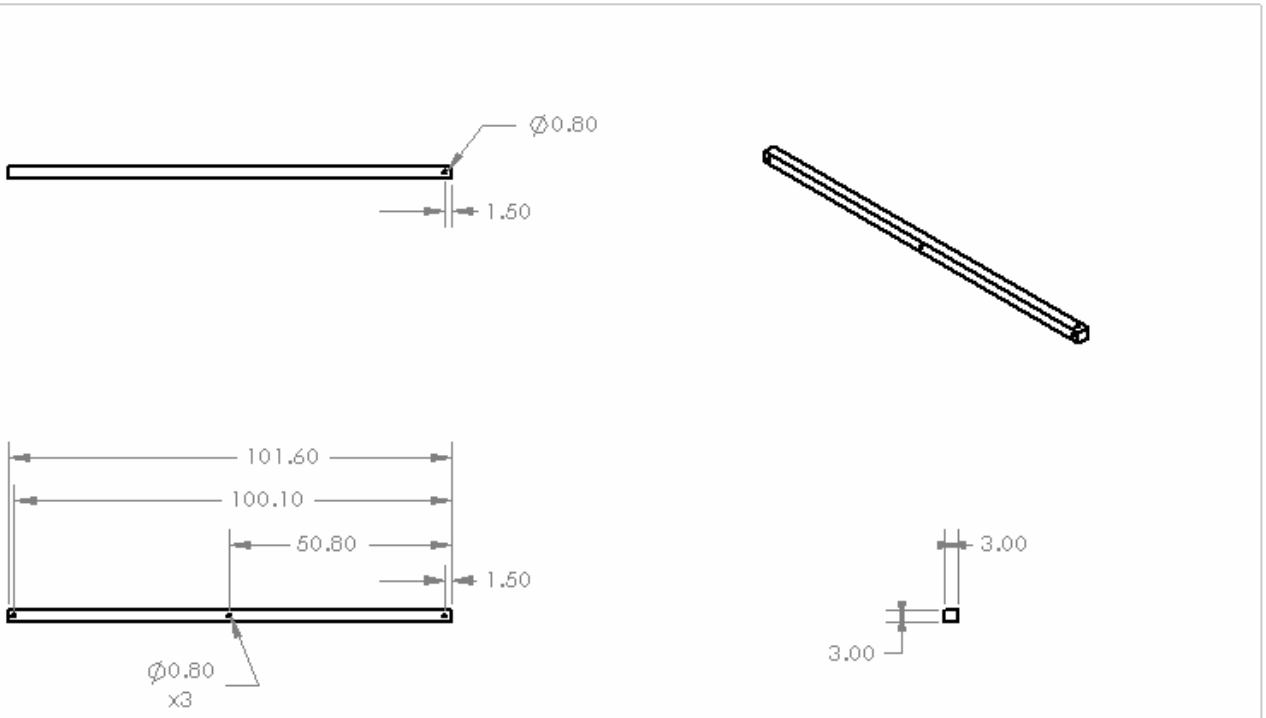

		UNLESS OTHERWISE SPECIFIED:		NAME	DATE
		DIMENSIONS ARE IN MM TOLERANCES: FRACTIONAL ± ANGULAR: MACH ± BEND ± TWO PLACE DECIMAL ± THREE PLACE DECIMAL ±	DRAWN		
			CHECKED		
			ENG APPR.		
			MFG APPR.		
			Q.A.		
		INTERPRET GEOMETRIC TOLERANCING PER:	COMMENTS:		
		MATERIAL			
NEXT ASSY	USED ON	FINISH			
APPLICATION		DO NOT SCALE DRAWING			

Gerald Lucas

TITLE:

SIZE	DWG. NO.	REV
A	B Beam	10/27/5
SCALE: 1:1	WEIGHT:	SHEET 1 OF 1

5 4 3 2 1

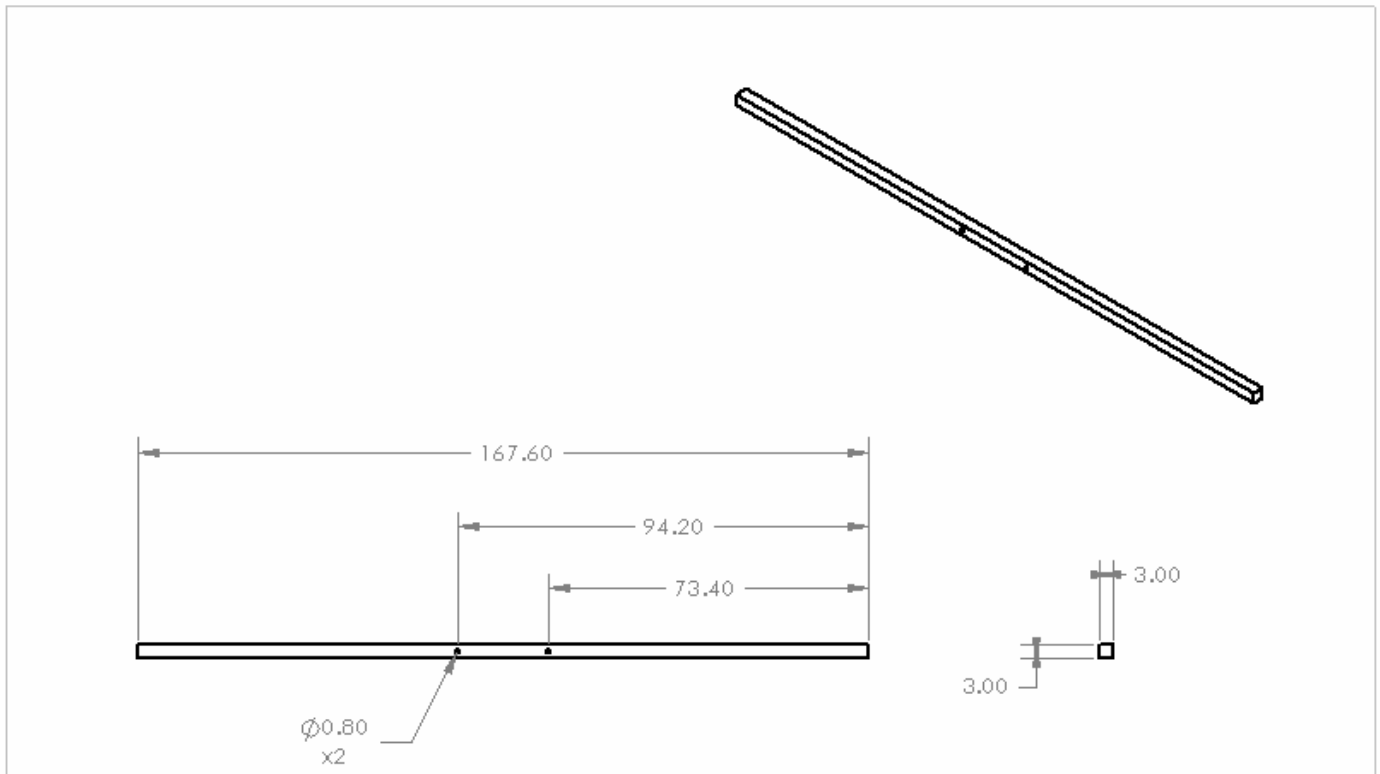

UNLESS OTHERWISE SPECIFIED:		NAME	DATE	Gerald Lucas	
DIMENSIONS ARE IN MM TOLERANCES: FRACTIONAL ± ANGULAR: MACH ± BEND ± TWO PLACE DECIMAL ±0.05 THREE PLACE DECIMAL ±	DRAWN			TITLE:	
	CHECKED				
	ENG APPR.				
	MFG APPR.				
	Q.A.				
INTERPRET GEOMETRIC TOLERANCING PER:	COMMENTS:			SIZE: A	DWG. NO.: C Beam
MATERIAL					REV: 10/27/5
FINISH				SCALE: 1:1	WEIGHT:
NEXT ASSY	USED ON				SHEET 1 OF 1
APPLICATION	DO NOT SCALE DRAWING				

5 4 3 2 1

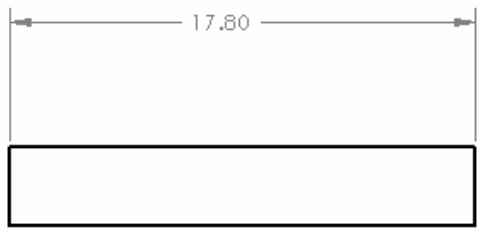

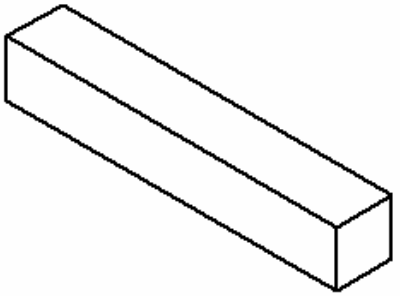

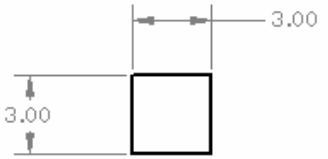

UNLESS OTHERWISE SPECIFIED:		NAME	DATE	Gerald Lucas	
DIMENSIONS ARE IN CM TOLERANCES: FRACTIONAL ± ANGULAR: MACH ± BEND ± TWO PLACE DECIMAL ± THREE PLACE DECIMAL ±	DRAWN			TITLE:	
	CHECKED				
	ENG APPR.				
	MFG APPR.				
	Q.A.				
INTERPRET GEOMETRIC TOLERANCING PER:	COMMENTS:			SIZE: A	DWG. NO.: F Beam
MATERIAL					REV: 10/27/5
FINISH					
NEXT ASSY	USED ON				
APPLICATION	DO NOT SCALE DRAWING			SCALE: 1:1	WEIGHT: SHEET 1 OF 1

5 4 3 2 1

3.00
3.00
161.60
UNLESS OTHERWISE SPECIFIED:
NAME
DATE
Gerald Lucas
DRAWN
CHECKED
ENG APPR.
MFG APPR.
Q.A.
COMMENTS:
TITLE:
SIZE
DWG. NO.
REV
A
Stabilizing
3/15/5
SCALE: 1:1
WEIGHT:
SHEET 1 OF 1

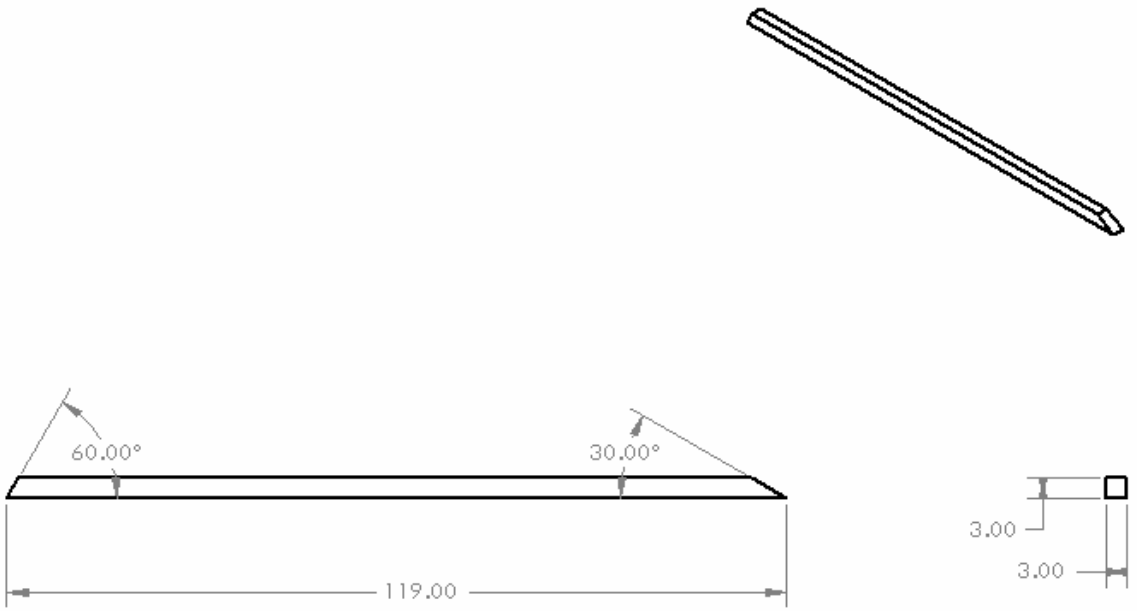

UNLESS OTHERWISE SPECIFIED:		NAME	DATE	Gerald Lucas	
DIMENSIONS ARE IN CM TOLERANCES: FRACTIONAL ± ANGULAR: MACH ± BEND ± TWO PLACE DECIMAL ± THREE PLACE DECIMAL ±	DRAWN			TITLE:	
	CHECKED				
	ENG APPR.				
	MFG APPR.				
	Q.A.				
INTERPRET GEOMETRIC TOLERANCING PER:	COMMENTS:			SIZE: A	DWG. NO.: Diagonal Beam
MATERIAL					REV: 3/15/6
FINISH					
NEXT ASSY	USED ON				
APPLICATION	DO NOT SCALE DRAWING			SCALE: 1:1	WEIGHT: SHEET 1 OF 1

5 4 3 2 1

ROTATOR

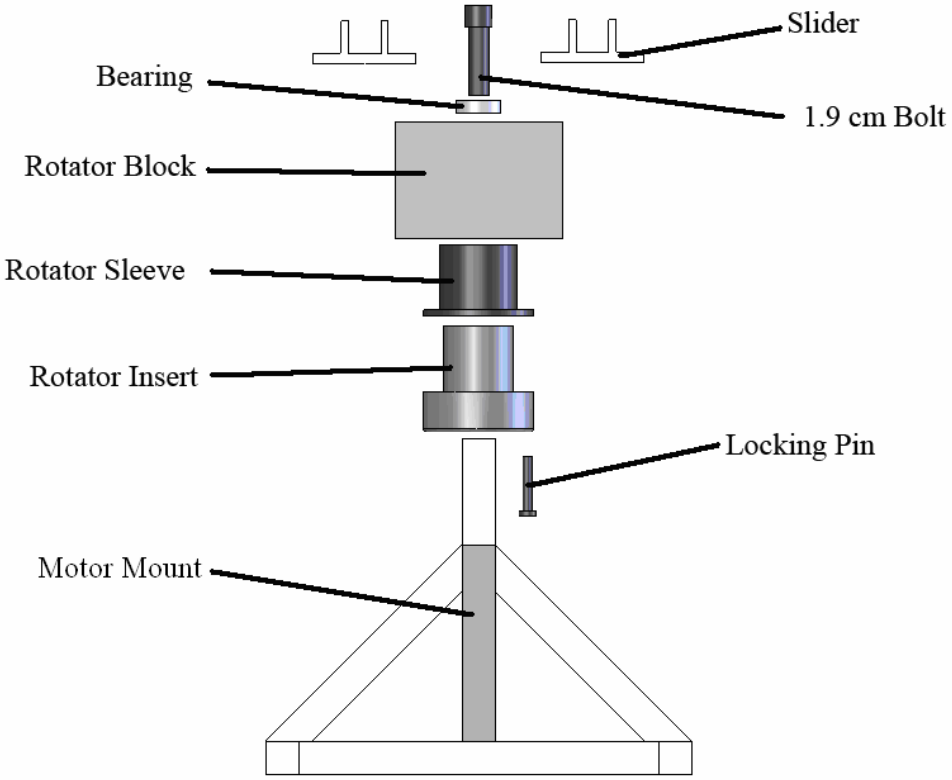
Slider
Bearing
1.9 cm Bolt
Rotator Block
Rotator Sleeve
Rotator Insert
Locking Pin
Motor Mount

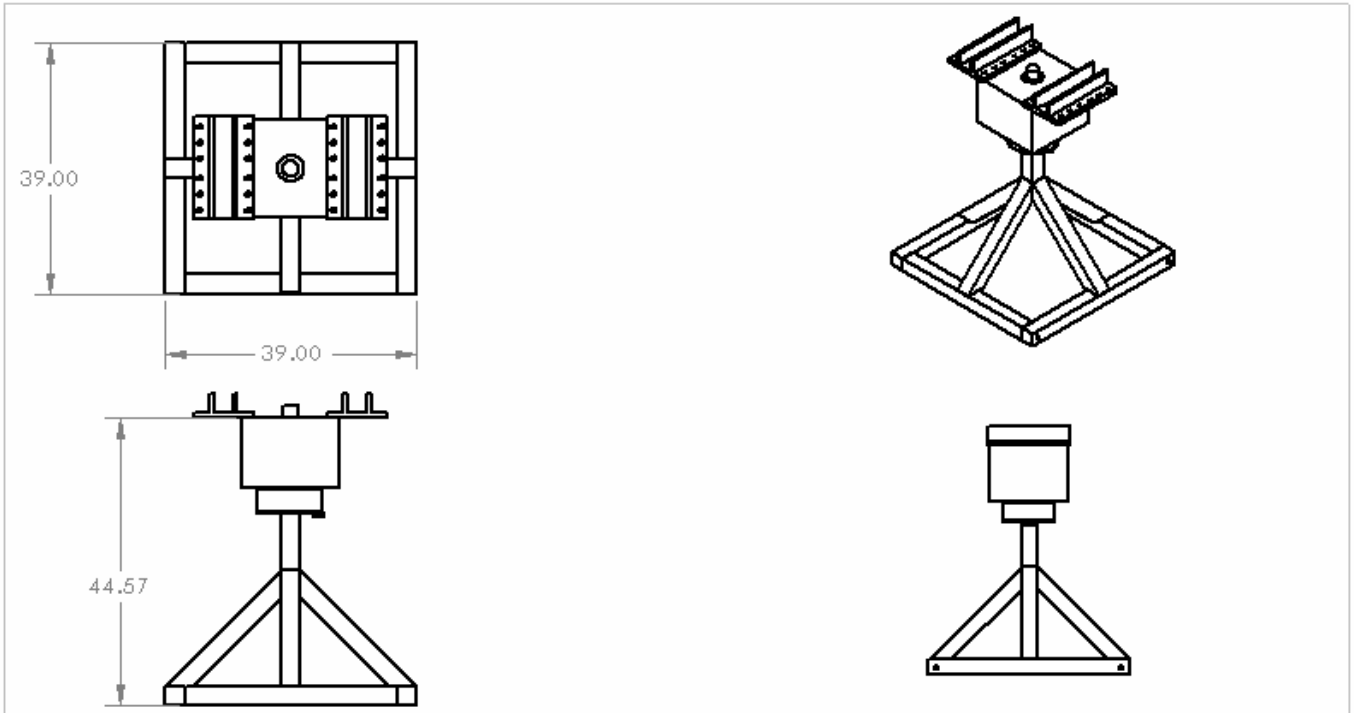

		UNLESS OTHERWISE SPECIFIED:		NAME	DATE
		DIMENSIONS ARE IN CM TOLERANCES: FRACTIONAL ± ANGULAR: MACH ± BEND ± TWO PLACE DECIMAL ± .20 THREE PLACE DECIMAL ±	DRAWN		
			CHECKED		
			ENG APPR		
			MFG APPR		
		INTERPRET GEOMETRIC TOLERANCING PER:	Q A		
		MATERIAL	COMMENTS:		
NEXT ASSY	USED ON	FINISH			
APPLICATION		DO NOT SCALE DRAWING			

Gerald Lucas

TITLE:

SIZE	DWG. NO.	REV
A	Rotator	9/25/6
SCALE 1:10	WEIGHT:	SHEET 1 OF 1

5 4 3 2 1

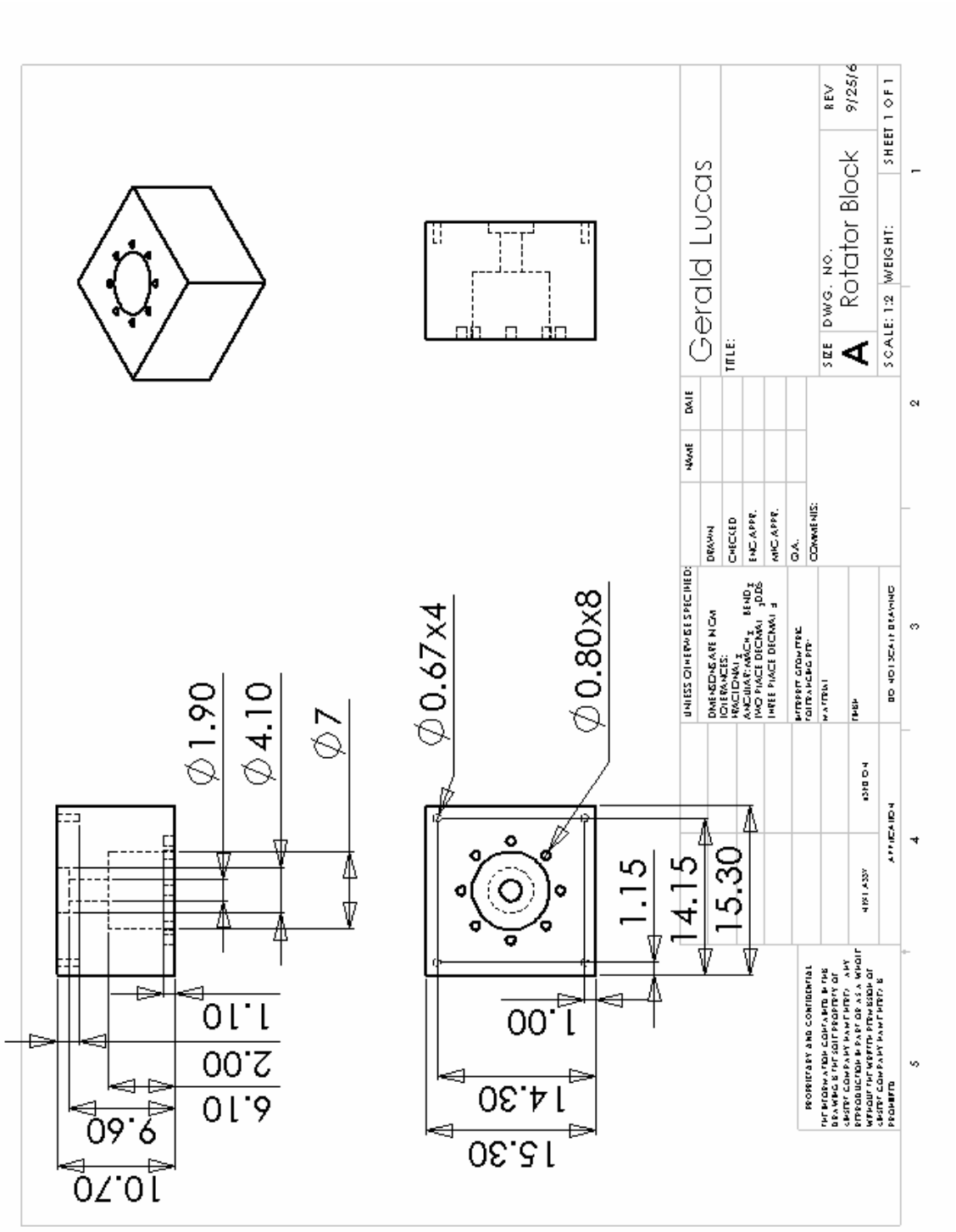
Gerald Lucas
Rotator Block
A
SIZE
DWG. NO.
REV
9/25/6
SCALE: 1:2
WEIGHT:
SHEET 1 OF 1
TITLE:
Ø1.90
Ø4.10
Ø7
10.70
9.60
6.10
2.00
1.10
Ø0.67x4
Ø0.80x8
15.30
14.30
1.00
1.15
14.15
15.30

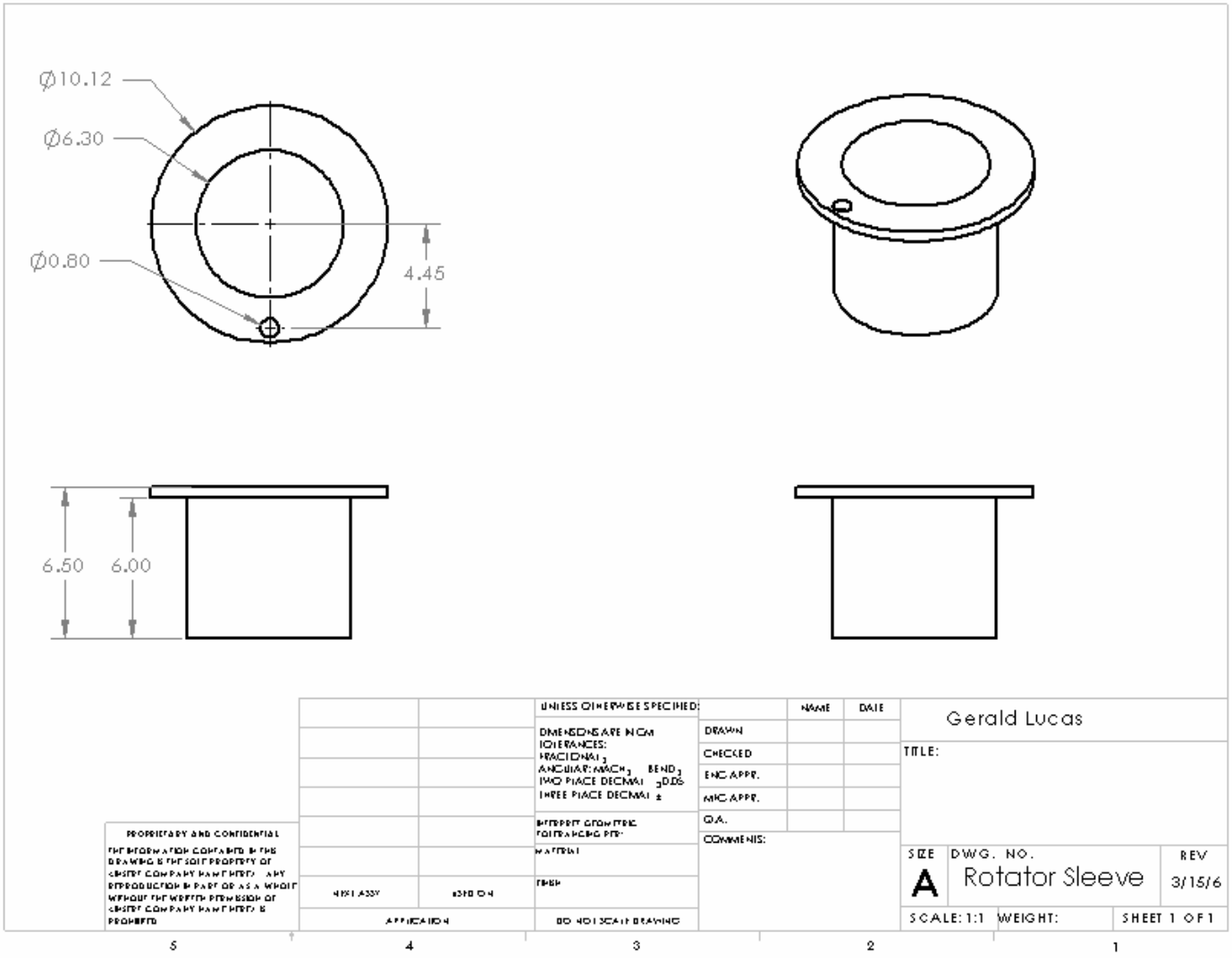
Ø10.12
Ø6.30
Ø0.80
4.45
6.50
6.00
UNLESS OTHERWISE SPECIFIED:
DIMENSIONS ARE IN CM
TOLERANCES:
FRACTIONAL ±
ANGULAR: MACH ± BEND ±
TWO PLACE DECIMAL ±0.05
THREE PLACE DECIMAL ±
INTERPRET GEOMETRIC TOLERANCING PER:
MATERIAL
FINISH
NEXT ASSY
USED ON
APPLICATION
DO NOT SCALE DRAWING
NAME
DATE
DRAWN
CHECKED
ENG APPR.
MFG APPR.
Q.A.
COMMENTS:
Gerald Lucas
TITLE:
SIZE
A
DWG. NO.
Rotator Sleeve
REV
3/15/6
SCALE: 1:1
WEIGHT:
SHEET 1 OF 1
PROPRIETARY AND CONFIDENTIAL
THE INFORMATION CONTAINED IN THIS DRAWING IS THE SOLE PROPERTY OF <INSERT COMPANY NAME HERE>. ANY REPRODUCTION IN PART OR AS A WHOLE WITHOUT THE WRITTEN PERMISSION OF <INSERT COMPANY NAME HERE> IS PROHIBITED.
5
4
3
2
1

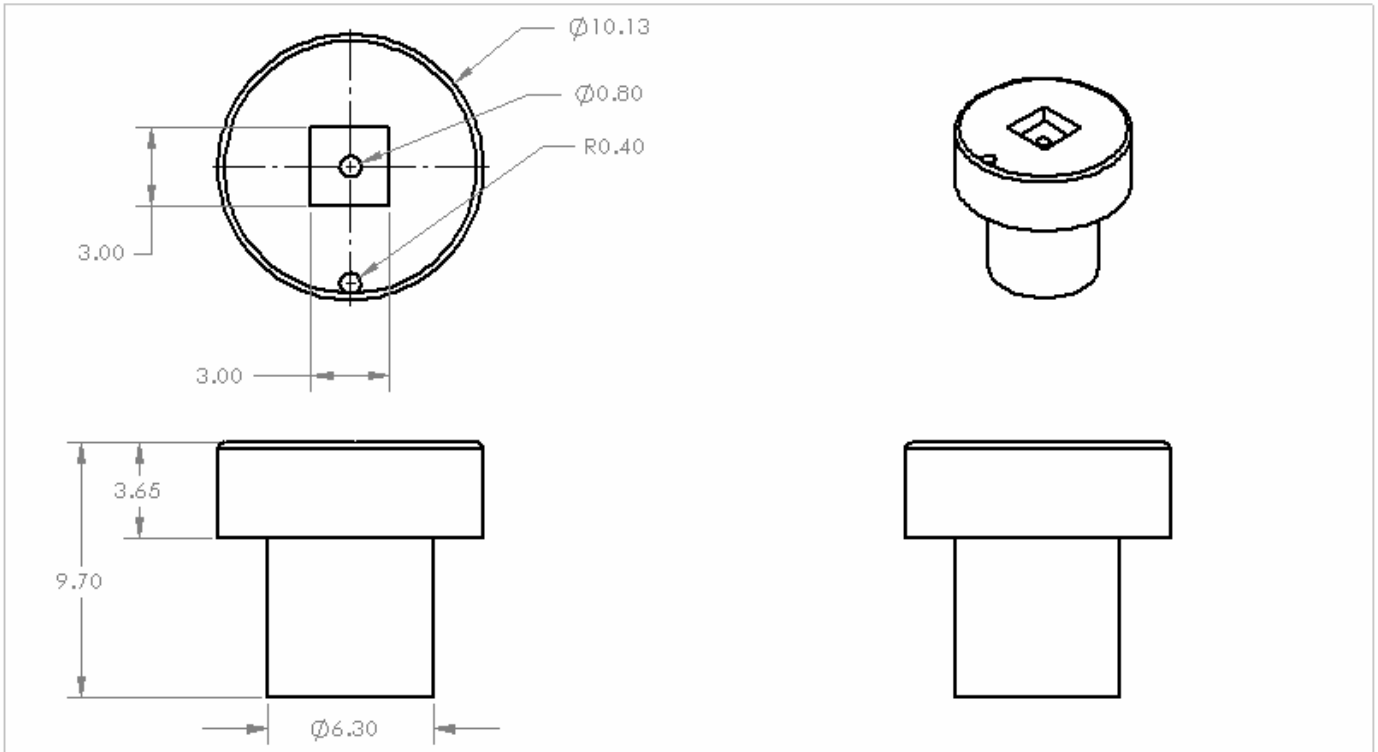

UNLESS OTHERWISE SPECIFIED:		NAME	DATE	Gerald Lucas	
DIMENSIONS ARE IN CM TOLERANCES: FRACTIONAL ± ANGULAR: MACH ± BEND ± TWO PLACE DECIMAL ±0.05 THREE PLACE DECIMAL ±	DRAWN			TITLE:	
	CHECKED				
	ENG APPR.				
	MFG APPR.				
INTERPRET GEOMETRIC TOLERANCING PER:	Q.A.				
MATERIAL	COMMENTS:			SIZE: A	DWG. NO.: Rotator Insert
FINISH					REV: 3/15/6
NEXT ASSY	USED ON				
APPLICATION	DO NOT SCALE DRAWING			SCALE: 1:1	WEIGHT: SHEET 1 OF 1

5 4 3 2 1

MOTOR MOUNT

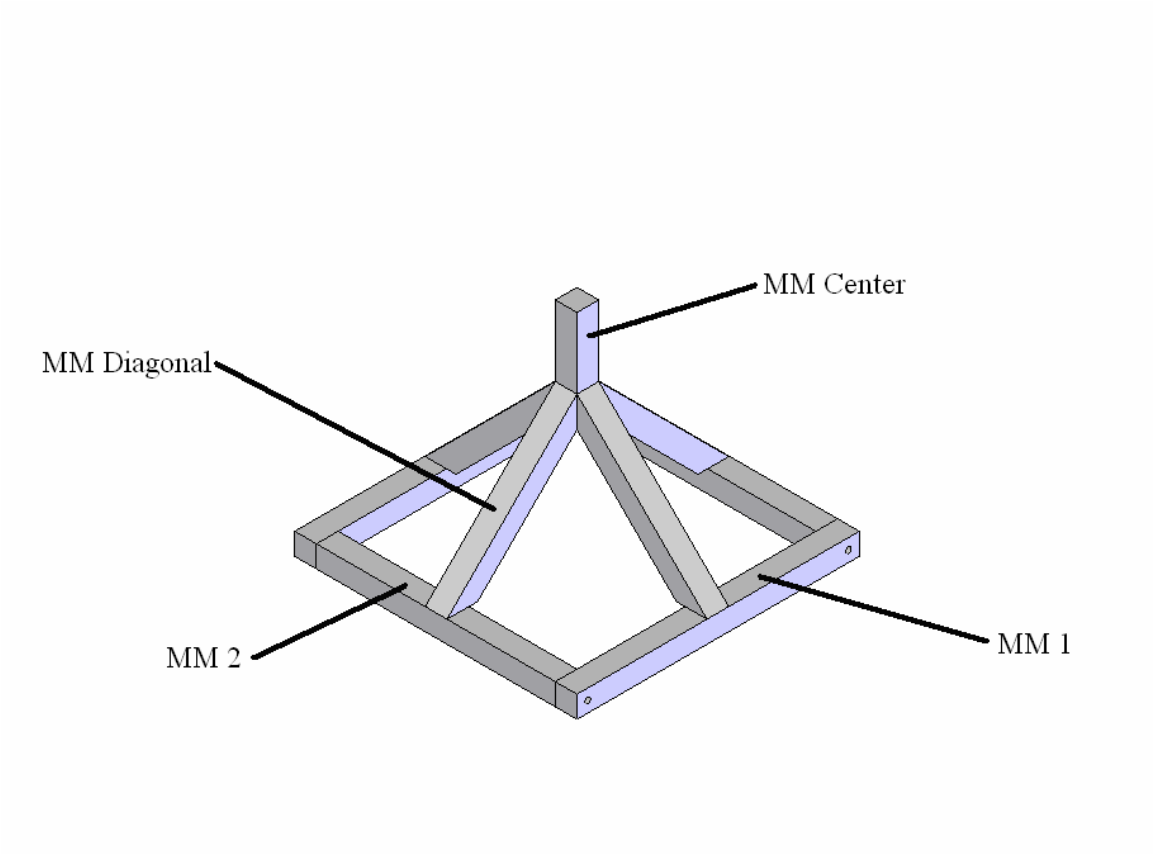

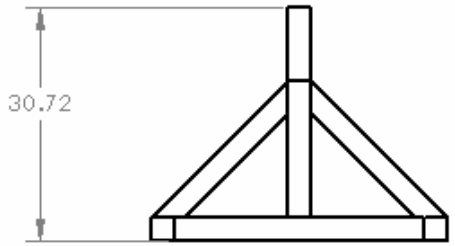

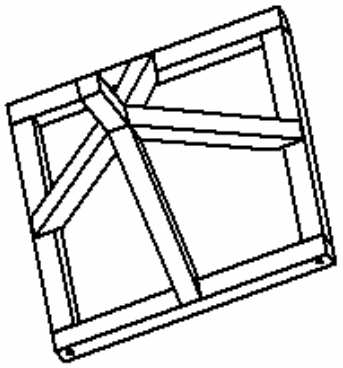

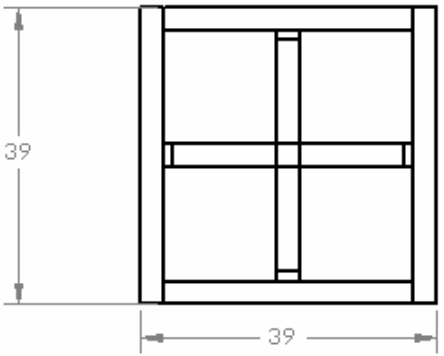

		UNLESS OTHERWISE SPECIFIED:		NAME	DATE
		DIMENSIONS ARE IN CM TOLERANCES: FRACTIONAL ANGULAR: MACH BEND ± TWO PLACE DECIMAL ±0.05 THREE PLACE DECIMAL ±	DRAWN		
			CHECKED		
			ENG APPR		
			MFG APPR		
		INTERPRET GEOMETRIC TOLERANCING PER:	Q A		
		MATERIAL	COMMENTS:		
		FINISH			
NEXT ASSY	USED ON				
APPLICATION		DO NOT SCALE DRAWING			

Gerald Lucas

TITLE:

SIZE	DWG. NO.	REV
A	MM	10/27/5
SCALE: 1:1	WEIGHT:	SHEET 1 OF 1

5 4 3 2 1

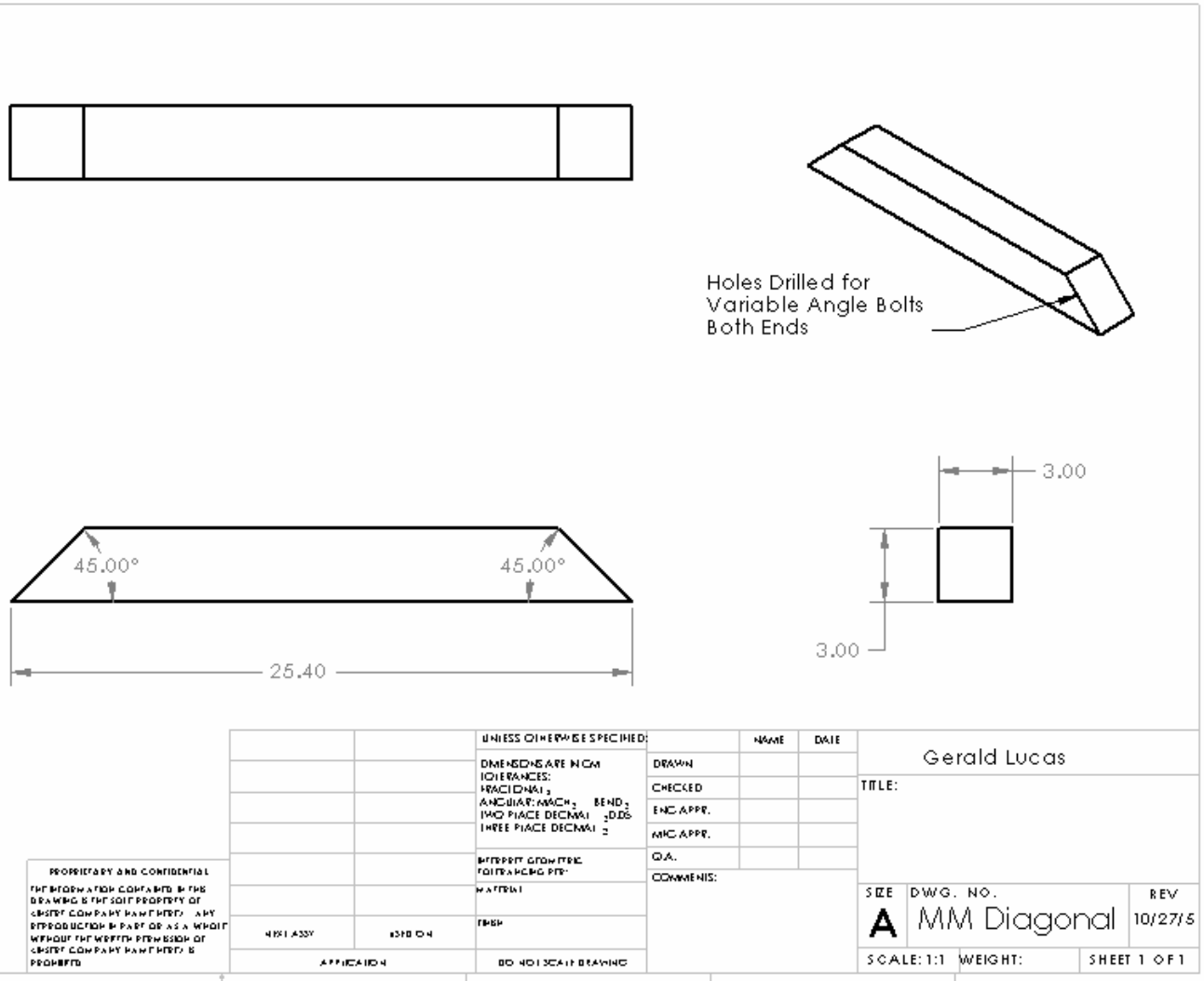

UNLESS OTHERWISE SPECIFIED:		NAME	DATE	Gerald Lucas	
DIMENSIONS ARE IN CM TOLERANCES: FRACTIONAL ± ANGULAR: MACH ± BEND ± TWO PLACE DECIMAL ±0.05 THREE PLACE DECIMAL ±	DRAWN			TITLE:	
	CHECKED				
	ENG APPR.				
	MFG APPR.				
	Q.A.				
INTERPRET GEOMETRIC TOLERANCING PER:	COMMENTS:			SIZE: A	DWG. NO.: MM Diagonal
MATERIAL					REV: 10/27/15
FINISH					
NEXT ASSY	USED ON				
APPLICATION	DO NOT SCALE DRAWING			SCALE: 1:1	WEIGHT: SHEET 1 OF 1

5 4 3 2 1

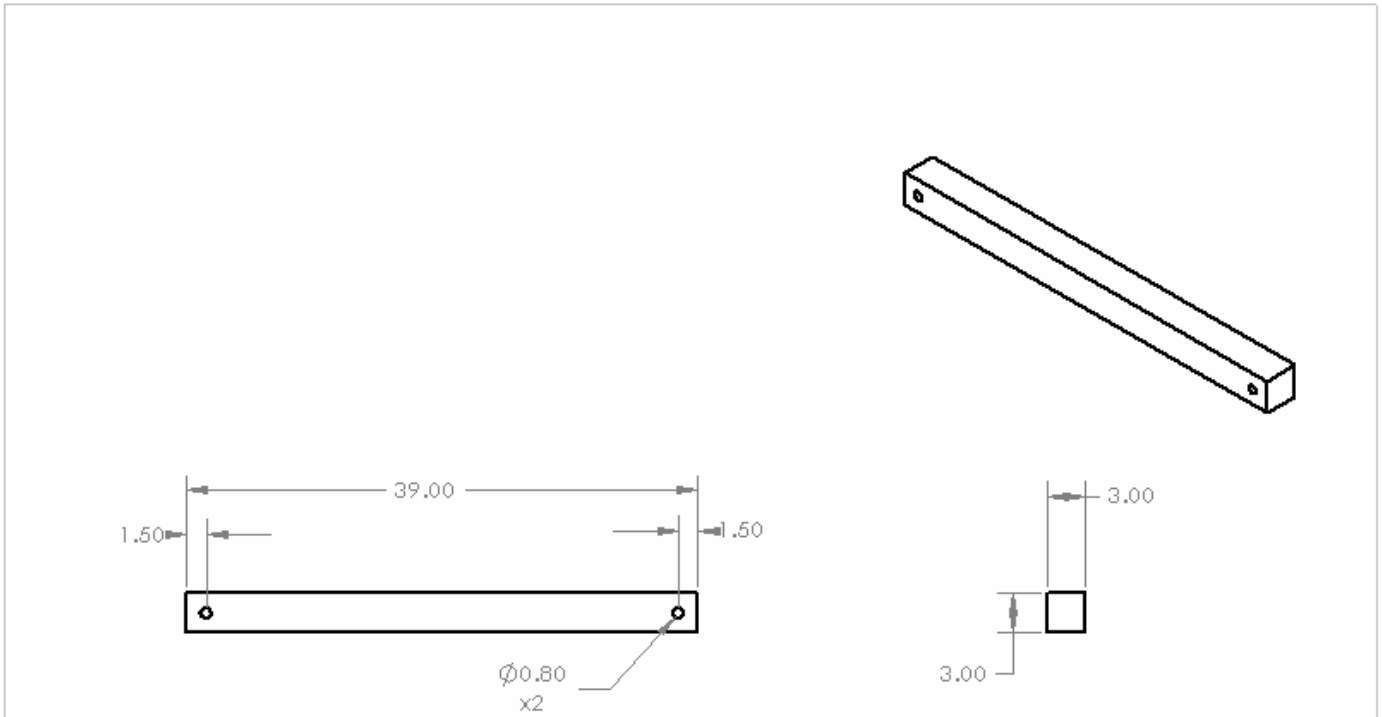

UNLESS OTHERWISE SPECIFIED:		NAME	DATE	Gerald Lucas	
DIMENSIONS ARE IN CM TOLERANCES: FRACTIONAL ± ANGULAR: MACH ± BEND ± TWO PLACE DECIMAL ±0.05 THREE PLACE DECIMAL ±	DRAWN			TITLE:	
	CHECKED				
	ENG APPR.				
	MFG APPR.				
	Q.A.				
INTERPRET GEOMETRIC TOLERANCING PER:	COMMENTS:			SIZE: A	DWG. NO.: MM1
MATERIAL					REV: 10/27/5
FINISH					
NEXT ASSY	USED ON				
APPLICATION	DO NOT SCALE DRAWING			SCALE: 1:1	WEIGHT: SHEET 1 OF 1

5 4 3 2 1

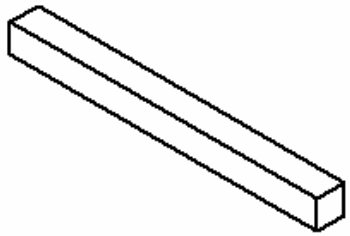

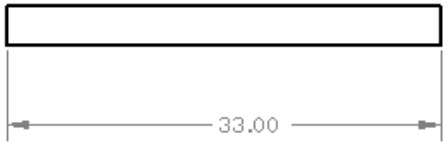

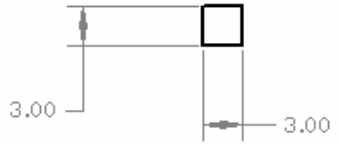

UNLESS OTHERWISE SPECIFIED:		NAME	DATE	Gerald Lucas	
DIMENSIONS ARE IN CM TOLERANCES: FRACTIONAL ± ANGULAR: MACH ± BEND ± TWO PLACE DECIMAL ±0.05 THREE PLACE DECIMAL ±	DRAWN			TITLE:	
	CHECKED				
	ENG APPR.				
	MFG APPR.				
	Q.A.				
INTERPRET GEOMETRIC TOLERANCING PER:	COMMENTS:			SIZE: A	DWG. NO.: MM2
MATERIAL					REV: 10/30/15
FINISH					
NEXT ASSY	USED ON				
APPLICATION	DO NOT SCALE DRAWING			SCALE: 1:1	WEIGHT: SHEET 1 OF 1

5 4 3 2 1

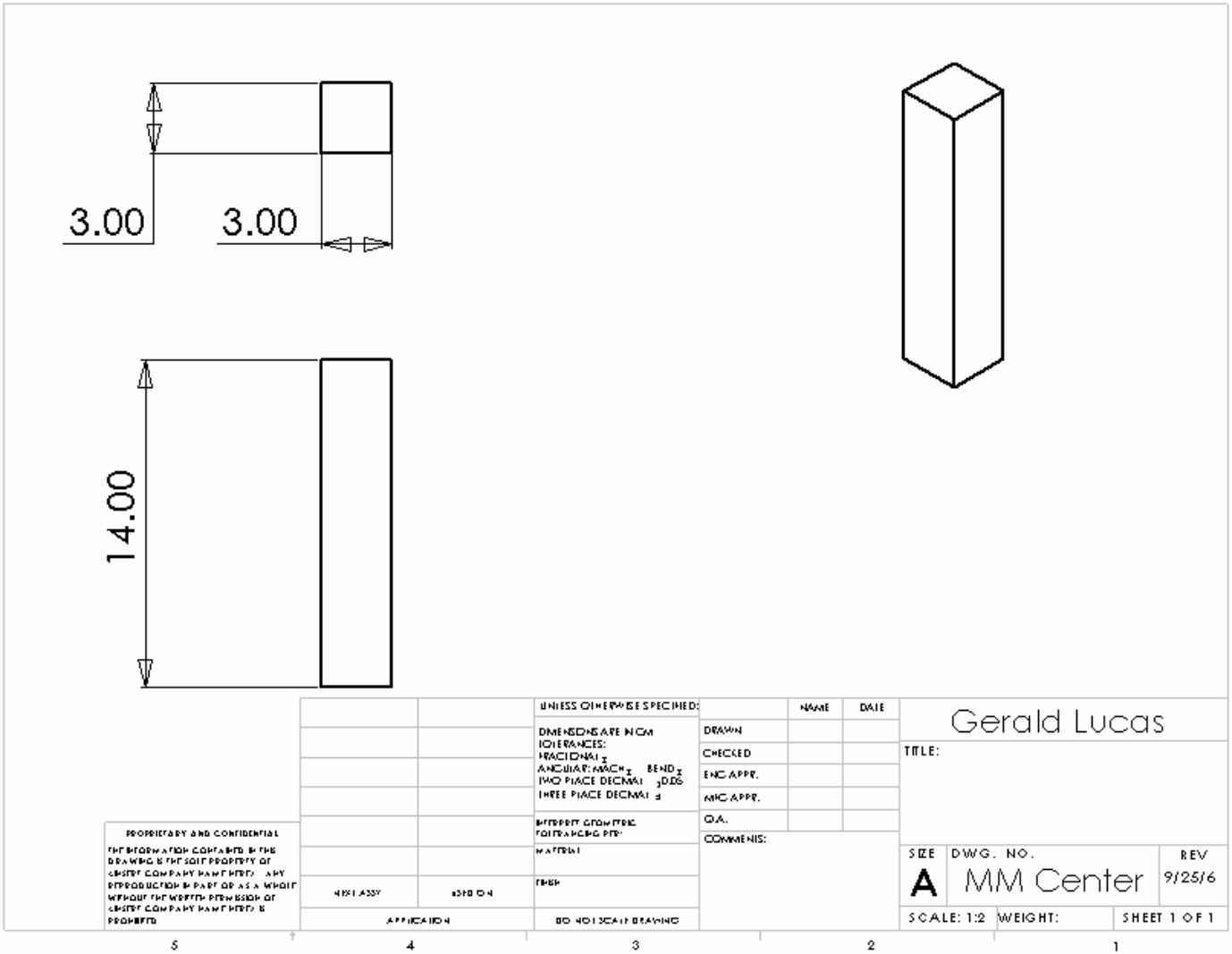
3.00
3.00
14.00
UNLESS OTHERWISE SPECIFIED:
NAME
DATE
DRAWN
CHECKED
ENG APPR.
MFG APPR.
Q.A.
COMMENTS:
Gerald Lucas
TITLE:
SIZE
A
DWG. NO.
MM Center
REV
9/25/6
SCALE: 1:2
WEIGHT:
SHEET 1 OF 1
PROPRIETARY AND CONFIDENTIAL
THE INFORMATION CONTAINED IN THIS DRAWING IS THE SOLE PROPERTY OF <INSERT COMPANY NAME HERE>. ANY REPRODUCTION IN PART OR AS A WHOLE WITHOUT THE WRITTEN PERMISSION OF <INSERT COMPANY NAME HERE> IS PROHIBITED
NEXT ASSY
USED ON
APPLICATION
DO NOT SCALE DRAWING
INTERPRET GEOMETRIC TOLERANCING PER:
MATERIAL
FINISH
DIMENSIONS ARE IN CM
TOLERANCES:
FRACTIONAL ±
ANGULAR: MACH ± BEND ±
TWO PLACE DECIMAL ±0.05
THREE PLACE DECIMAL ±
5
4
3
2
1